



National Library  
of Canada

Bibliothèque nationale  
du Canada

Canadian Theses Service

Service des thèses canadiennes

Ottawa, Canada  
K1A 0N4

## NOTICE

The quality of this microform is heavily dependent upon the quality of the original thesis submitted for microfilming. Every effort has been made to ensure the highest quality of reproduction possible.

If pages are missing, contact the university which granted the degree.

Some pages may have indistinct print especially if the original pages were typed with a poor typewriter ribbon or if the university sent us an inferior photocopy.

Reproduction in full or in part of this microform is governed by the Canadian Copyright Act, R.S.C. 1970, c. C-30, and subsequent amendments.

## AVIS

La qualité de cette microforme dépend grandement de la qualité de la thèse soumise au microfilmage. Nous avons tout fait pour assurer une qualité supérieure de reproduction.

S'il manque des pages, veuillez communiquer avec l'université qui a conféré le grade.

La qualité d'impression de certaines pages peut laisser à désirer, surtout si les pages originales ont été dactylographiées à l'aide d'un ruban usé ou si l'université nous a fait parvenir une photocopie de qualité inférieure.

La reproduction, même partielle, de cette microforme est soumise à la Loi canadienne sur le droit d'auteur, SRC 1970, c. C-30, et ses amendements subséquents.

THE UNIVERSITY OF ALBERTA

Deformation Pulses Recorded by Sediment Accumulation in the  
Cordilleran Foreland Basin, Peace River Arch Area, Alberta

by

James R. Underschultz



A THESIS

SUBMITTED TO THE FACULTY OF GRADUATE STUDIES AND RESEARCH  
IN PARTIAL FULFILMENT OF THE REQUIREMENTS FOR THE DEGREE  
OF MASTER OF SCIENCE

Department of Geology

EDMONTON, ALBERTA

Spring, 1990

## NOTICE

The quality of this microform is heavily dependent upon the quality of the original thesis submitted for microfilming. Every effort has been made to ensure the highest quality of reproduction possible.

If pages are missing, contact the university which granted the degree.

Some pages may have indistinct print especially if the original pages were typed with a poor typewriter ribbon or if the university sent us an inferior photocopy.

Reproduction in full or in part of this microform is governed by the Canadian Copyright Act, R.S.C. 1970, c. C-30, and subsequent amendments.

## AVIS

La qualité de cette microforme dépend grandement de la qualité de la thèse soumise au microfilmage. Nous avons tout fait pour assurer une qualité supérieure de reproduction.

S'il manque des pages, veuillez communiquer avec l'université qui a conféré le grade.

La qualité d'impression de certaines pages peut laisser à désirer, surtout si les pages originales ont été dactylographiées à l'aide d'un ruban usé ou si l'université nous a fait parvenir une photocopie de qualité inférieure.

La reproduction, même partielle, de cette microforme est soumise à la Loi canadienne sur le droit d'auteur, SRC 1970, c. C-30, et ses amendements subséquents.

ISBN 0-315-60309-7

THE UNIVERSITY OF ALBERTA

RELEASE FORM

NAME OF AUTHOR: JAMES R. UNDERSCHULTZ


TITLE OF THESIS: DEFORMATION PULSES RECORDED BY SEDIMENT  
ACCUMULATION IN THE CORDILLERAN FORELAND BASIN, PEACE  
RIVER ARCH AREA, ALBERTA

DEGREE: MASTER OF SCIENCE

YEAR THIS DEGREE GRANTED: 1990

Permission is hereby granted to THE UNIVERSITY OF  
ALBERTA LIBRARY to reproduce single copies of this thesis  
and to lend or sell such copies for private, scholarly,  
or scientific research purposes only.

The author reserves other publication rights, and  
neither the thesis nor extensive extracts from it may  
be printed or otherwise reproduced without the author's  
written permission.



PO box 75

Beaumont Alberta, Canada.

TOC OH0

Date: Feb 27/90

THE UNIVERSITY OF ALBERTA

FACULTY OF GRADUATE STUDIES AND RESEARCH

The undersigned certify that they have read, and recommend to the Faculty of Graduate Studies and Research for acceptance, a thesis entitled Deformation Pulses Recorded by Sediment Accumulation in the Cordilleran Foreland Basin, Peace River Arch Area, Alberta submitted by James R. Unterschultz in partial fulfilment of the requirements for the degree of Master of Science.

*Philippe Eschen*

.....

(Supervisor)

*John Holdsworth*

.....

*S. E. Roberts*

.....

*J. A. K. Chalcraft*

.....

.....

FEB 15 1990

Date: .....

## ABSTRACT

Rates of mass accumulation calculated for Cretaceous units in the Cordilleran foreland basin can be categorized into three groups based on their magnitude. These groups of low, moderate, and high rates of accumulation can be related to deformation events in the Canadian Cordillera. When the rates of accumulation are organized on an absolute time scale, they show a distinct cyclic pattern.

From early Aptian to late Campanian time, there were two major episodes of mountain building, each preceded by a period of relative quiescence. The first episode lasted from 113 to 108 MaBP. It shows a succession of rapid, moderate, and rapid deformational events, with durations of approximately 1, 2, and 2 Ma, respectively. The second episode of deformation lasted from 94 to 87 MaBP and is characterized by three periods of rapid deformational events separated by short intervals of quiescence. The rapid deformation events have durations of 0.5, 4.5, and 1.0 Ma whereas the periods of quiescence lasted 0.5 Ma each. This cyclic pattern may be related to fundamental convergent tectonic processes.

## ACKNOWLEDGMENTS

I would like to acknowledge, with appreciation, Dr. P. Erdmer for his assistance and encouragement during the preparation of this thesis. I would also like to recognize the support of the Alberta Geological Survey of the Alberta Research Council, in particular Dr. S. Bachu and Dr. J.A. Boon.

## TABLE OF CONTENTS

Chapter	Page
1. INTRODUCTION .....	1
2. PREVIOUS WORK .....	3
3. STUDY AREA .....	7
4. PROCEDURE AND BACKGROUND INFORMATION .....	9
A. DATA .....	10
Geology Data .....	10
Core Data .....	14
B. MAPPING PROCEDURES AND TECHNIQUES .....	15
Porosity Maps .....	16
Solid Thickness Maps .....	18
Grain Density Maps .....	18
Mass Accumulation Rate Maps .....	18
5. ABSOLUTE AGE AND STRATIGRAPHIC CORRELATION .....	21
6. MASS ACCUMULATION RATES .....	29
A. COMPARISON WITH ISOPACHS .....	30
7. INTERPRETATIONS .....	33
A. FERNIE GROUP .....	33
B. BULLHEAD GROUP .....	34
C. BLUESKY FORMATION .....	36
D. LOWER SPIRIT RIVER GROUP .....	36
E. UPPER SPIRIT RIVER GROUP .....	36
F. LOWER PEACE RIVER GROUP .....	38
G. UPPER PEACE RIVER GROUP .....	38
H. SHAFTESBURY FORMATION .....	41
I. DUNVEGAN FORMATION .....	41



J. LOWER KASKAPAU FORMATION .....	43
K. DOE CREEK FORMATION .....	43
L. UPPER KASKAPAU FORMATION .....	43
M. CARDIUM FORMATION .....	45
N. MUSKIKI FORMATION .....	45
O. BADHEART FORMATION .....	45
P. LOWER PUSKWASKAU FORMATION .....	47
Q. CHINOOK FORMATION .....	47
R. UPPER PUSKWASKAU FORMATION .....	47
8. DISCUSSION .....	51
A. CYCLIC NATURE OF DEFORMATION .....	51
B. PREDICTIONS ARISING FROM THE OBSERVED CYCLES .....	55
C. DEFORMATION AND LITHOLOGY .....	56
D. MODEL OF TECTONIC DEVELOPMENT .....	58
9. CONCLUSIONS .....	62
10. REFERENCES .....	65
11. APPENDIX A .....	68
12. APPENDIX B .....	77

## LIST OF TABLES

Table	Page
1. Generalized chronostratigraphic nomenclature distilled from D. Stott (personal communication 1989) and Davies (1984) .....	23
2. Synthesized stratigraphic correlation (after D. Stott, personal communication 1989) .....	24
3. Absolute age and mass accumulation rate data for all units .....	52

## LIST OF FIGURES

Figure	Page
1. Peace River Arch study area and the Phanerozoic isopach for the Western Canada Sedimentary Basin ....	8
2. Data distribution for the entire geological data base .....	11
3. Data distribution for core analysis in the Bluesky Formation .....	12
4. Upper Spirit River Group. (a) Porosity (%); (b) Solid Thickness (m) .....	17
5. Upper Spirit River Group. (a) Grain Density ( $\text{kg/m}^3$ ); (b) Mass accumulation rate ( $\text{kg/m}^2/\text{Ma} \times 10^3$ ) .....	19
6. Lower Peace River Group. (a) Isopach (m); (b) Mass accumulation rate ( $\text{kg/m}^2/\text{Ma} \times 10^3$ ) .....	31
7. Mass accumulation rate ( $\text{kg/m}^2/\text{Ma} \times 10^3$ ). (a) Fernie Group; (b) Bullhead Group .....	35
8. Mass accumulation rate ( $\text{kg/m}^2/\text{Ma} \times 10^3$ ). (a) Bluesky Formation; (b) Lower Spirit River Group .....	37
9. Mass accumulation rate ( $\text{kg/m}^2/\text{Ma} \times 10^3$ ). (a) Upper Spirit River Group; (b) Lower Peace River Group .....	39
10. Mass accumulation rate ( $\text{kg/m}^2/\text{Ma} \times 10^3$ ). (a) Upper Peace River Group; (b) Shaftesbury Formation .....	40

11. Mass accumulation rate ( $\text{kg/m}^2/\text{Ma} \times 10^3$ ). (a) Dunvegan Formation; (b) Lower Kaskapau Formation .....	42
12. Mass accumulation rate ( $\text{kg/m}^2/\text{Ma} \times 10^3$ ). (a) Doe Creek Formation; (b) Upper Kaskapau Formation .....	44
13. Mass accumulation rate ( $\text{kg/m}^2/\text{Ma} \times 10^3$ ). (a) Cardium Formation; (b) Muskiki Formation .....	46
14. Mass accumulation rate ( $\text{kg/m}^2/\text{Ma} \times 10^3$ ). (a) Badheart Formation; (b) Lower Puskwaskau Formation .....	48
15. Mass accumulation rate ( $\text{kg/m}^2/\text{Ma} \times 10^3$ ). (a) Chinook Formation; (b) Upper Puskwaskau Formation .....	49
16. Plot of accumulation rate versus time .....	52
17. Schematic diagram indicating the six main phases of deformation undergone by the northern Canadian Cordillera .....	59

## 1. INTRODUCTION

The Canadian Cordillera developed as a result of a complex history of terrane accretion and deformation along the western edge of the North American craton. Since mid-Jurassic time, western North America has been under the influence of a convergent tectonic regime which has dominated geological processes (Monger, 1984). With the onset of convergence, the passive margin, previously dominated by carbonate deposition, changed to a site of active deformation which initiated a foreland phase of basin development. As foreign terranes impinged on the craton they exerted a downward force, causing crustal flexure. Sediments were eroded from the new relief in the west and shed eastward, filling the downflexed foreland basin. To date, much of the effort in trying to understand the history of Cordilleran development has been concentrated on the study of the Cordillera itself. This has provided explanations of the mechanisms and structural styles of deformation, but has only broadly defined the location and age of deformation events. The present study was undertaken with the purpose of constraining deformation events in both time and space, by attempting to quantify the sedimentary response in the foreland basin.

The approach taken is to consider mass accumulation rates for a selected number of geological units. This requires isopach, time zonation, grain density, and porosity data. The distribution of accumulation rate provides information on the provenance of sediment and the general environment of deposition. From these distributions it is apparent that the locus of deformation migrates along the Cordillera

over time, and can be very localized or very broad. When mass accumulation rate is plotted against absolute time, a cyclic pattern of deformation emerges.

As the initial unit thickness dominates mass accumulation rate, the accuracy of the study results are limited by the confidence placed in the biostratigraphic delineation of the basin as defined by public data. When a more accurate basin geometry is available, the error in the study results may be reduced. A different approach, that of defining the geological framework by sequence stratigraphy, may prove to be beneficial in analyzing mass accumulation rates. To date, this approach has been applied by other workers only on a few select stratigraphic intervals such as within the Cardium and Viking Formations. Within an individual stratigraphic horizon this approach to characterizing the sediments leads to quite different correlations than determined by the lithostratigraphic approach. However, it is unclear how significant these detailed internal discrepancies will be when scaled up to the dimensions of the basin.

## 2. PREVIOUS WORK

Numerous researchers have described the structural and stratigraphic framework of the Cordillera at different scales. In a recent overview, Monger (1984) suggested that the tectonic development of the Canadian Cordillera is the result of a series of terrane accretion events. Radiometric dating of intrusives within the Omineca Crystalline belt and Coast Plutonic Complex has led to estimates for the time of accretion of two Cordilleran Superterrane (late Early to Middle Jurassic and mid Cretaceous); however, the history of accretion and subsequent deformation is still unclear, and there are only general estimates for the timing and location of deformation events.

Geodynamic basin modelers such as Bird (1978), Beaumont (1981), Jordan (1981), England (1982), and Stockmal (1984), have developed models which predict the formation and filling of basins resulting from the load exerted by terrane accretion and thrust-fold belt development. As a deformation history incorporating the location and magnitude of deformation events is not available, basin modelers have taken the approach of backward modeling. This is where the existing geometry of the foreland basin is examined, and an iterative series of loading "scenarios" are tested until the model reflects present-day geometry (Beaumont, 1981). Because present day geometry can be obtained by several different loading histories, this procedure sheds little new light on the actual deformation history.

A foreland basin which forms adjacent to newly developing convergent margins acts as a tape recorder of orogenic deformation. As new relief is generated in the deformed belt, erosion supplies a pulse

of sediment to the downflexed foreland basin which, if preserved, records that deformation interval. Puigdefabregas *et al.* (1986) noted that sedimentation in the Southern Pyrenees Foreland basin could be linked to three deformational events in the eastern Pyrenees. Johnson *et al.* (1986) examined sediment accumulation in the northwestern Himalayan foredeep in the Potwar region and were able to define the onset, duration, and termination of two major deformation intervals. Eisbacher *et al.* (1974) made one of the first attempts to associate the history of sedimentation in the western Canadian foreland basin with deformation in the Cordillera. Tankard (1986) related foreland basin sedimentation to three stages of Cordilleran development. An initial pulse of sediment was deposited during late Jurassic and early Cretaceous time as terranes were accreted on the edge of the previously passive margin. A period of tectonic quiescence accompanied the mid-Cretaceous deposition of thick marine shales. Finally, upper Cretaceous sands and coals were deposited as Laramide thrusting emplaced loads on thermally mature continental crust causing the basin to oscillate between overfilled and starved conditions. Cant and Stockmal (1989) have related specific clastic wedges to individual terrane accretion events in the Canadian Cordillera. Thus, most attempts at linking sedimentation in the foreland basin to deformation in the Canadian Cordillera have been based on the geometry of clastic wedges and the lithology of the sediment.

Another, more quantitative approach to characterizing the sediment in the foreland basin is to calculate sedimentation rates. Turcotte (1980), Watts *et al.* (1982), and Guidish *et al.* (1984) studied the subsidence of a basin as a result of sediment deposition and sea



level change. Sedimentation rates can be used to estimate loads on the lithosphere over time and to quantify the sedimentary response to deformation in the adjacent Cordillera. The approach used is to first define specific units and display them by means of isopach maps. The units are then decompacted to their original depositional thickness, and divided by the time interval they represent (Magara, 1978). The resultant sedimentation rate can be related to deformation in the Cordillera. However, lateral tectonic stresses, rebound from unloading, local zones of overpressure, and changes in rock type are uncontrolled variables that introduce a large uncertainty in the final results (Pate, 1986), making it unreliable for interpreting Cordilleran deformation. In the Western Canada Sedimentary Basin these problems are compounded by the existence of several major unconformities, the erosional magnitude of which is not precisely known. The decompaction process is applied in one dimension, making it difficult to get a basin-wide characterization of sedimentation rates. The sedimentation rate method is required if the sediment load on the lithosphere is to be known, because the water-filled porosity contributes significantly to the total load. For this study, the primary interest is in the change of sedimentation with time; therefore, porosity can be neglected, and decompaction difficulties avoided, by calculating mass accumulation rates rather than sedimentation rates.

Mass accumulation rates reflect the provenance of the sediment, the general environment of deposition, and the location and magnitude of tectonic activity in the adjacent deformed belt. Maps of mass accumulation rate are more reliable than those of sedimentation rate because the former only require geological characterization and core

analysis data, which are directly measurable and readily available. The use of mass accumulation rates eliminates the need to estimate burial histories.

It is assumed that deformation in the Cordillera generates relief which in turn increases the rate of erosion. If the material is being removed from the Cordillera at an increased rate there will be a corresponding increase in the rate of sediment accumulation in the adjacent foreland basin. Between Aptian and Campanian times there are no major unconformities within the study area which influence the calculation of mass accumulation rates. Beaumont (1981), has shown that eustatic sea level fluctuation has only second order effects on basin geometry and these effects are observed on the eastern feather edge of the basin where a sea level change can significantly move the shoreline. These effects occur east of the study area and are not considered in the calculation of mass accumulation rates. Therefore, changes in the rate of accumulation of foreland basin sediment can be related to equivalent changes in the rate of deformation in the Cordillera.

### 3. STUDY AREA

In order to take advantage of work in progress characterizing the subsurface geology, the study area selected is that of the Peace River Arch Study Area described by the Basin Analysis and Petroleum Geology Group of the Alberta Geological Survey. The study area, covering part of northwest Alberta and northeast British Columbia, is from 54° to 58°N and 114° to 124°W (Figure 1). It is extensive enough to permit recognition of the migration of Cordilleran source regions. Stratigraphically, the foreland basin is represented by post-Triassic units of dominantly sand and shale, recording approximately 208 Ma of the basin's history.

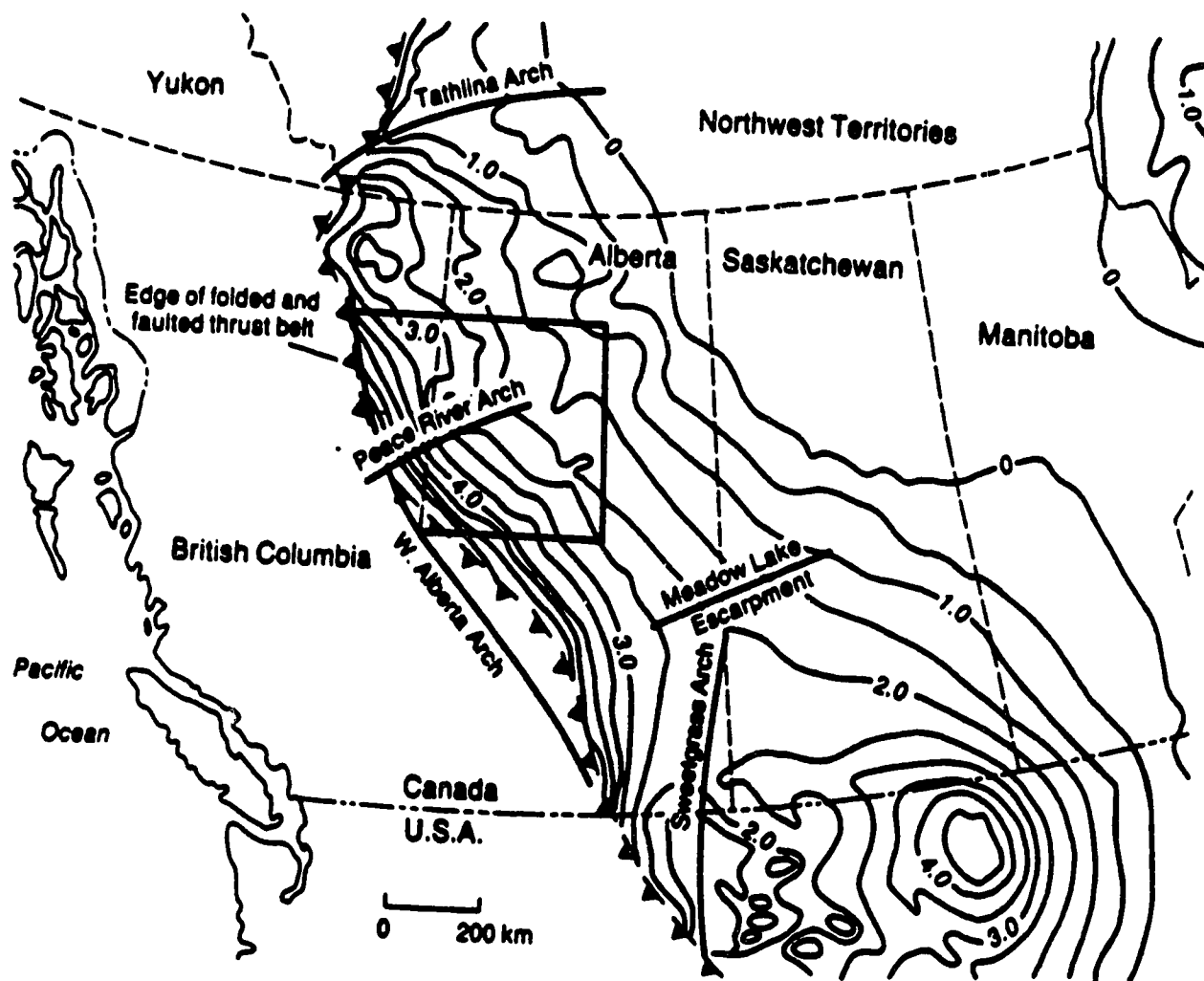


Figure 1. Peace River Arch study area and the Phanerozoic isopach for the Western Canada Sedimentary Basin.

#### 4. PROCEDURE AND BACKGROUND INFORMATION

In order to obtain a mass accumulation rate  $R_m$  for a specific rock unit, its thickness ( $Q$ ) is multiplied by one minus its porosity ( $n$ ) to give solid thickness  $Q_s$ :

$$Q_s = Q (1 - n)$$

The solid thickness is multiplied by its density ( $\rho$ ) and divided by a representative time interval ( $T$ ), to give a mass accumulation rate with units of mass/unit-area/Ma.

$$R_m = \frac{(Q_s \times \rho)}{T}$$

This is a measure of how quickly a particular unit accumulated in the basin.

For the Western Canada Sedimentary Basin, isopach, porosity, and solid rock density data are available from the Alberta Energy Resources Conservation Board (ERCB) well data base. Therefore, all parameters used to calculate the mass accumulation rates are easily accessible and directly measurable.

The following sections describe the data, processing, and methods used in mapping various parameters in the Peace River Arch study area.

## A. DATA

Three data sets are required: 1) The **geological data set** (Figure 2) contains the location of wells and the elevations of the geological picks made from geophysical logs; the isopachs of each of the geological units are derived from this data set (see Appendix A); 2) The **porosity data** can be obtained either from standard core analysis or calculated from drill stem tests; core analysis data were used in this study due to their large number and accessibility (see appendix B); 3) The **solid grain density data** were obtained from standard core analysis reports (Appendix B). Figure 3 shows an example of the core analysis data distribution for the Bluesky Formation.

### Geological Data

Nineteen units were defined, using two separate data bases. The Alberta Geological Survey Well Data Base (AGSWDB) is derived from ERCB-picks, and contains stratigraphic information for wells drilled within Alberta. The Peace River Arch Well Data Base (PRAWDB) contains stratigraphic picks specific to the project study area, at a density of at least one well per township where data is available. The PRAWDB was derived by the Petroleum Geology and Basin Analysis group of the Alberta Research Council from manual log analysis. The AGSWDB is generally of poorer quality than the PRAWDB due to lack of consistency in the picking procedure; however, it has much higher data density, and for specific horizons the quality is comparable to that of the PRAWDB. The ERCB tends to accumulate stratigraphic data over time, all of which

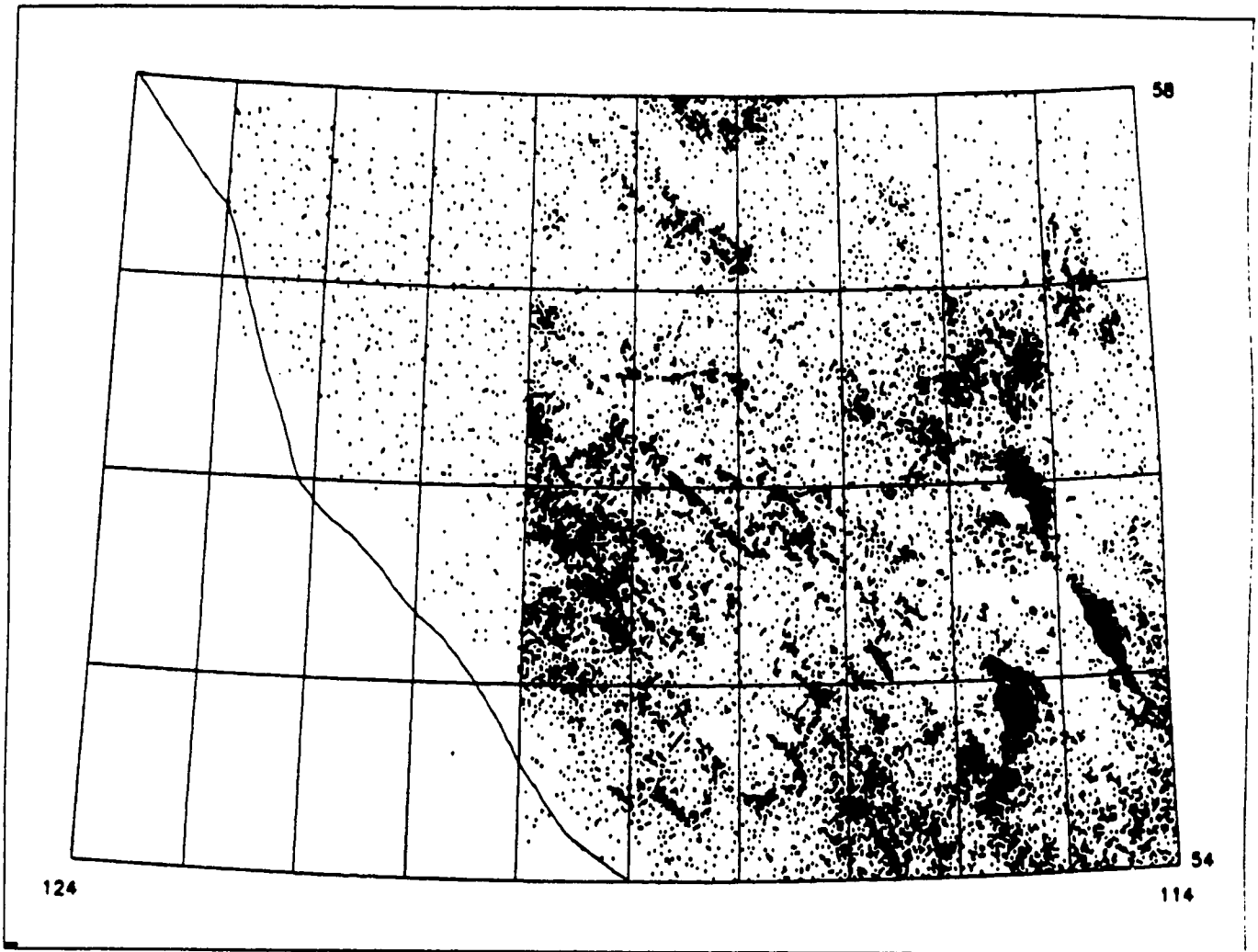


Figure 2. Data distribution for the entire geological data base.

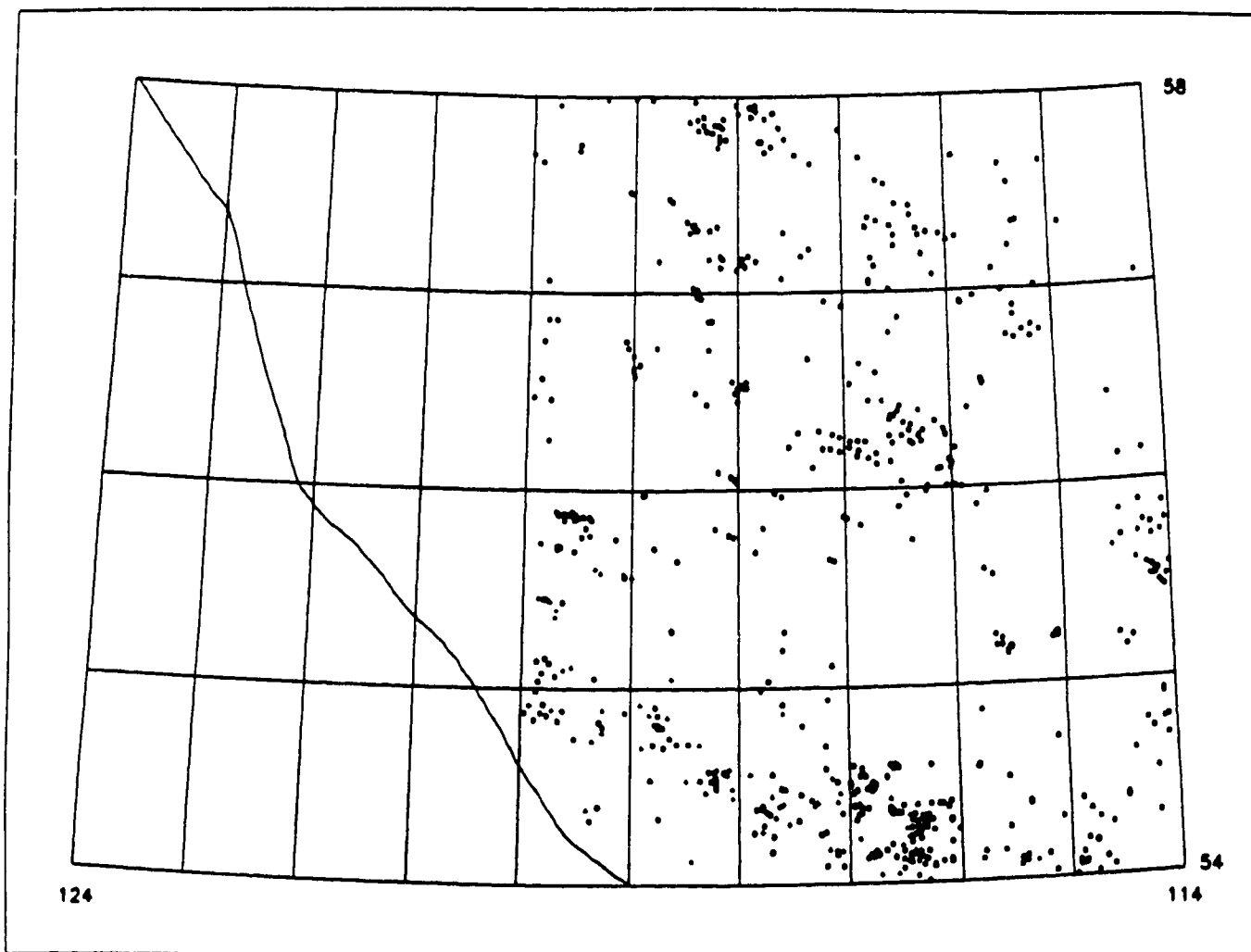


Figure 3. Data distribution for core analysis in the Bluesky Formation.



is stored in the general well data base. The sources of contributions to this data base have varied over time, with several ERCB employees picking stratigraphic tops for any particular horizon. This method of data collection has inherent inconsistencies in interpretations of geophysical logs by various workers. The inconsistencies vary in their magnitude depending on the complexity of the stratigraphic correlation in question. For example, the Nordegg Formation has a distinctive signature on geophysical logs because it is the first regional carbonate unit at the base of a clastic sequence of sand and shale. In contrast, the Muskiki Formation is a shale-dominated unit bounded by both shale and sand-dominated units. Its signature is not as distinct as that of the Nordegg Formation because the contrast in rock type from adjacent units is not as strong, and different observers may use different log responses to define it. The PRAWDB contains information gathered by individuals dedicated to specific stratigraphic horizons, thus ensuring correlations within the study area to be consistent.

On the basis of data consistency and complexity of correlation, horizons were selected for which data in both data bases were of comparable quality; these are the top of the Nordegg Formation and the present day ground surfaces. Because the Nordegg Formation subcrops at the pre-Cretaceous unconformity, it was combined with the pick for the top of the unconformity and mapped as a single lower bounding surface. Present ground level and the top of the Nordegg Formation form the upper and lower bounding surfaces, and being defined by both data sets, they are constrained by a large number of control points (ground surface (21,841) and Nordegg (12,396)). The units between the ground and Nordegg surfaces are defined by data from the PRAWDB only; the

AGSWDB was not used because of the inconsistency of the ERCB data.

Structure surfaces for each of the units were constructed using the stratigraphic picks data. Isopachs were generated by subtracting the structure surface at the base of a unit from the structure surface defining the top of the unit.

#### Core Data

The core data consist of a series of core analyses at various elevations for each land location. The parameters used are solid grain density and porosity, which are recorded routinely during standard core analysis. These data are part of the ERCB data base and are included in the core analysis section of the AGSWDB. For the Alberta portion of the Peace River Arch area, all the core analyses were extracted and allocated to the geological units defined for the foreland basin. There were no data available in electronic form from the British Columbia portion of the study area, and entering the hard copy data would have been too time consuming for the purposes of this project. For this reason, no core analysis data from British Columbia were used.

Both solid grain density and porosity measurements were made for each plug within cored intervals, and thus represent a point value in three-dimensional space. As a result, there are commonly several measurements recorded within a unit at the same land location. In order to get a map of the solid grain density or porosity for each unit, vertical averaging was used. The data were separated into files for each unit and then all values within each unit which had the same land location were arithmetically averaged. As a core analysis is

representative for a specific section of the total cored interval, and as the data are scalar (i.e., not spatially dependent), a weighted arithmetic average was selected over other averaging procedures. This ensured that the final data set contained only a single value for each land location in each geologic unit. These data are amenable to mapping. Core data was chosen over log analysis techniques in order to avoid biases introduced by individual interpretations of log data.

## B. MAPPING PROCEDURES AND TECHNIQUES

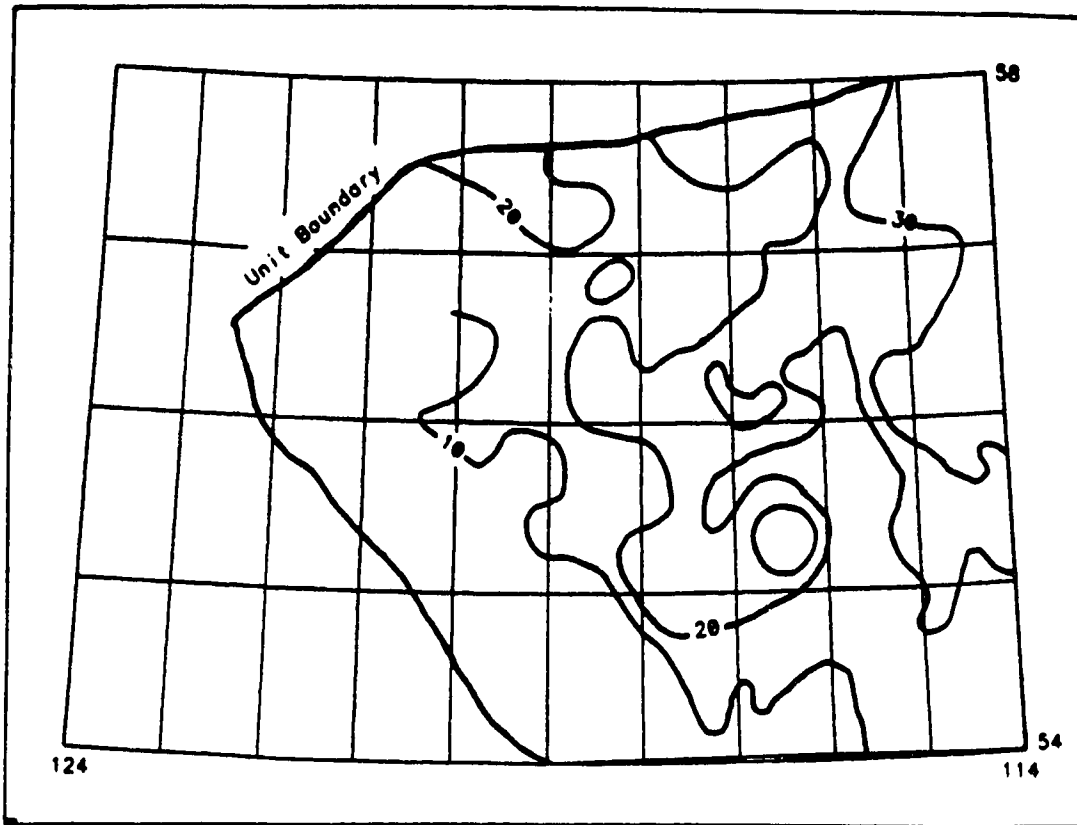
The process of producing a map can be divided into two stages. The first stage, gridding, is the transformation of an irregular data distribution into a regular distribution of grid nodes. The second stage is contouring the grid. All grids and maps were produced using the SURFACE II software (Sampson 1978) implemented on the Alberta Research Council computer system. The selected gridding algorithm calculates a first-order trend surface at each of the data points, which is fitted to the nearby data points found within a specified search radius. The trend surface is made to pass through the data point, thus becoming a least-squares estimate of the dip of the surface at that data point. The dips from all the data points within the search radius are then projected onto the grid node in question, using a distance weighted average, and a value is calculated. The approach used is described by Bachu *et al.* (1987) and is similar for all data types. A minimum of 3 and a maximum of 6 data points were required within a 10 node search radius in order to assign a value to a grid node.

The geological maps must be compatible (i.e. may not intersect) in three dimensions. To ensure compatibility, the ground and Nordegg surfaces (defined by the greatest number of points, and considered most reliable) are designated as "control surfaces". These surfaces are taken to be correct even where unconstrained. All surfaces which fall between the control surfaces are checked against one another to ensure that they do not intersect. In the event of an intersection, individual grid nodes for that surface are modified to fit between neighboring surfaces using grid manipulation software. The control surfaces remain unaltered. Isopach grids are generated by subtracting the structure grid of a unit's base from the structure grid of the unit's top.

#### Porosity Maps

Porosity maps such as that for the Upper Spirit River Group (Figure 4a) were created from vertically averaged core data for all 19 units listed in Table 1 with the exception of the Puskawaskau, Shaftesbury, Lower Peace River and Lower Spirit River units, which did not contain sufficient data to be gridded. In the absence of measured data an assumed trend surface was used as a default. The assumed porosity trend was calculated by averaging porosity trends from other shale-dominated units. The resultant surface permits an estimate of mass accumulation rates based on inferred porosity.

(a)



(b)

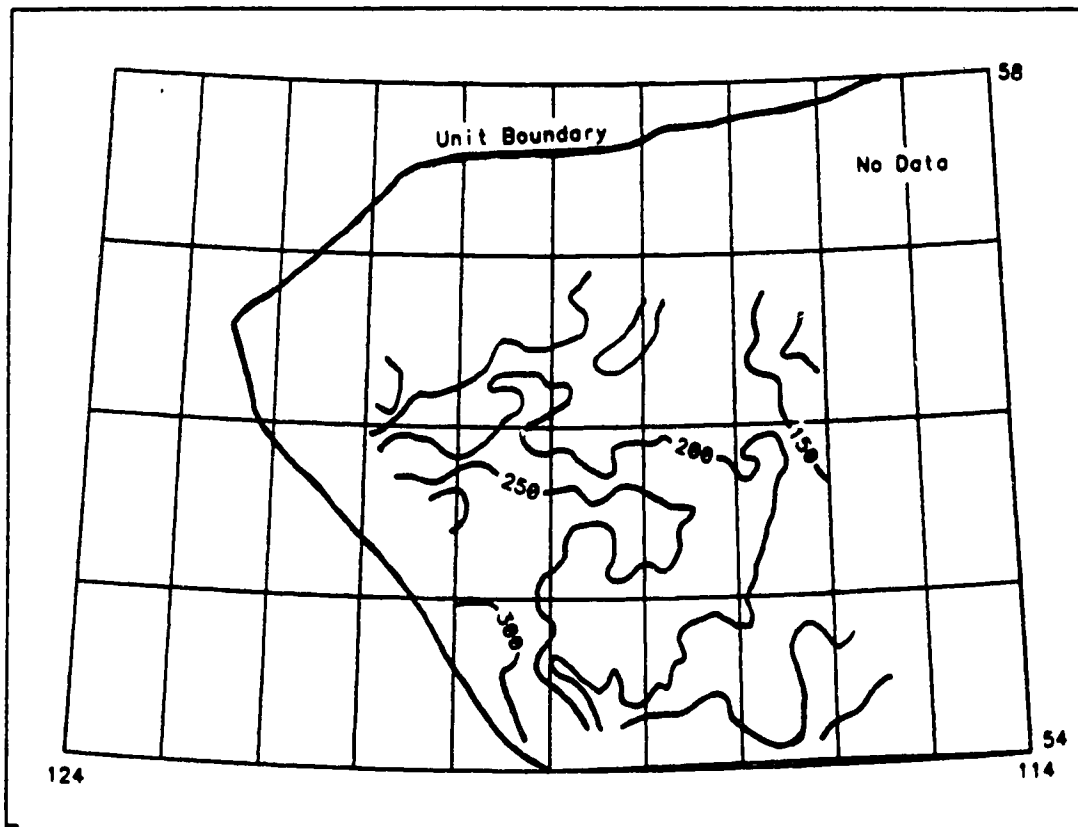


Figure 4. Upper Spirit River Formation. (a) Porosity (%);  
(b) Solid thickness (m).

### Solid Thickness Maps

A solid thickness contour is the equivalent of an isopach with the porosity contribution removed. A computer program was used which takes the isopach and porosity grids for each unit and multiplies the isopach value by one minus the porosity value at each node in the grid. The result is a grid of the solid thickness (Figure 4b). In the case of the Puskawaskau, Shaftesbury, Lower Peace River, and Lower Spirit River units, the default porosity trend surface was used.

### Grain Density Maps

The grain density data were mapped (Figure 5a) in a similar fashion to the porosity data. There are no grain density data for the Puskawaskau, Shaftesbury, Lower Peace River, and Lower Spirit River units. Because none of the grain density maps showed a distinctive trend (based on a Piersons correlation coefficient between density and land location), a default density value of  $2664 \text{ kg/m}^3$  was used, obtained by averaging densities of other shale units. This value was used to estimate mass accumulation rates for the units lacking density data.

### Mass Accumulation Rate Maps

The mass accumulation rate maps were produced using the solid thickness grids, the estimate of absolute age, and the density grids or default values. A computer program was used which reads the solid

(a)



(b)

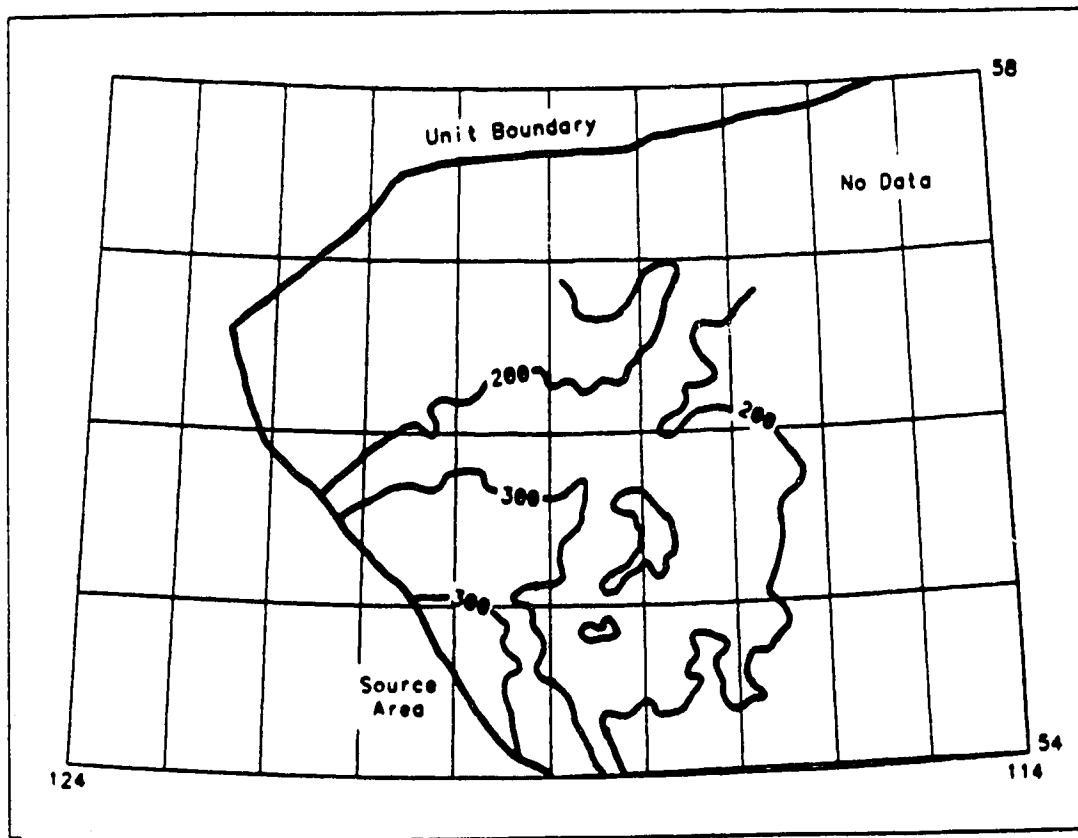


Figure 5. Upper Spirit River Formation. (a) Grain density ( $\text{kg/m}^3$ );  
 (b) Mass accumulation rate ( $\text{kg/m}^2/\text{Ma} \times 10^3$ ).

thickness grid, the density grid or default value, and the time interval. For each node, it multiplies the solid thickness value by the density value, and divides by the specified time interval. It stores the result in a mass accumulation rate grid which is then contoured (Figure 5b).



## 5. ABSOLUTE AGE AND STRATIGRAPHIC CORRELATION

An absolute age was assigned to the top and base of each of the nineteen units shown in Table 1. The absolute time scale of Kent and Gradstein (1985) was combined with the stratigraphic correlation charts of D. Stott (personal communication 1989) and Davies (1986) in order to estimate appropriate absolute ages for the units within the study area. The Kent and Gradstein time scale (1985) was selected as it is the most recent published update of Palmer's (1983) time scale. The stratigraphic correlation chart (Table 2) from Stott shows a selected number of areas of post-Triassic strata which are pertinent to the Peace River Arch study area. This compilation was selected in order to take advantage of the most recent correlation updates and biostratigraphic zonation. The correlations in Table 2 were supplemented by correlations of Davies (1986) then distilled into a single chronostratigraphic nomenclature for the entire study area (Table 1).

The Kent and Gradstein (1985) time scale has stage boundary dates based on a variety of dating methods. From Kimmeridgian to Barremian, and from Campanian to Maastrichtian stages, the absolute age estimates are based on an age-calibrated sea-floor spreading model. Kent and Gradstein (1985) used published isotopic age determinations for Aptian to Santonian stage boundaries; Hettangian to Oxfordian stage boundaries were estimated assuming equal duration of biozones. Based on this assumption, the absolute age of each biomarker is calculated from the nearest absolute age date determined by a method such as isotopic analysis.

**Table 1.** Generalized chronostratigraphic nomenclature. Distilled from D. Stott (personal communication 1989) and Davies (1986).

The Upper Puskwaskau Formation in Table 1 is that portion on the Puskwaskau Formation which overlies the Chinook Formation. The Chinook Formation does not appear in the Stott correlation; however, Davies (1986) shows the Chinook Formation in a chronostratigraphic interval equivalent to the Chungo Formation which Stott positions within, and near the top of the Puskwaskau Formation. The Lower Puskwaskau Formation of Table 1 is that portion of the Puskwaskau Formation which occurs between the base of the Chinook Formation and the top of the Badheart Formation. From Stott's correlation (Table 2) the Puskwaskau Formation in the Foothills belt is equivalent to the Upper Smokey Group in the Swan Hills region. Similarly, the Muskiki and Kaskapau Formations in the foothills are equivalent to the Middle and Lower Smokey Groups respectively. The Upper Kaskapau Formation on Table 1 refers to the portion of the Kaskapau which overlies the Doe Creek Formation. The Doe Creek Formation was positioned within the Kaskapau Formation following Davies (1986). The Lower Kaskapau Formation, which is not labeled due to space constraints on Table 1, is that portion of the Kaskapau which lies between the base of the Doe Creek Formation and the top of the Dunvegan Formation. The Upper Peace River Group on Table 1 is equivalent to the Cadotte and Boulder Creek formations of Stott (Table 2) and the Paddy and Cadotte formations of Davies (1986). The Lower Peace River Group from Table 1 is equivalent to the Harmon and Hulcross formations of Stott (Table 2). Similarly the Upper Spirit River is equivalent to the Notikewin/Falher and Gates formations from Table 2, and the Lower Spirit River Group is equivalent to the Wilrich and Moosebar formations. The Bullhead Group of Table 1 is the equivalent of the Gething and Cadomin formations of Stott (Table 2). The Nordegg which Stott only recognizes in the eastern Alberta foothills column of his correlation, was mapped regionally across the study area and is therefore considered to represent the Sinemurian for the Peace River Arch study area.

PEACE RIVER ARCH STUDY AREA	CHRONOSTRATIGRAPHIC UNITS		
UNIT NAME	SERIES/STAGE	AGE	SYSTEM
	MAASTRICHTIAN	66.4	CRETACEOUS
		74.5	
U. PUSKWASKAU CHINDOK	CAMPANIAN		
L. PUSKWASKAU		84.0	
BADHEART	SANTONIAN		
PUSKIKI		87.5	
CARILEP	CONIACIAN		
U. KASKAPAN DOX CREEK	TURONIAN		
DURVEGAN		91.0	
	CENOPIANIAN		
SHAFTESBURY		97.5	CRETACEOUS
	ALBIAN		
U. PEACE RIVER			
L. PEACE RIVER			
U. SPIRIT RIVER			
L. SPIRIT RIVER WILSON			
BULLHEAD	APTIAN	113.0	
		119.0	
	BARREMIAN		
	HAUTERIVIAN	124.0	
		131.0	
	VALANGINIAN		
	BERRIASIAN	138.0	
		144.0	JURASSIC
	TITHONIAN		
		152.0	
	KIMMERIDGIAN		
		156.0	
	OXFORDIAN		
		163.0	
	CALLOVIAN		
		169.0	
	BATHONIAN		
		176.0	
	BAJOCIAN		
		183.0	
	ALENIAN		
		187.0	
	TOARCIAN		
		193.0	
	PLIENSBAICHIAN		
		198.0	
	SINEMURIAN		
NORDEGG		204.0	
	HETTANGIAN	208.0	

Table 1. Generalized chronostratigraphic nomenclature.

PEACE RIVER ARCH			PEACE RIVER PLAINS		E ALBERTA FOOTHILLS		CHRONOSTRATIGRAPHIC UNITS		
PINE PASS	FT ST JOHN	SWAN MILLS	BRULÉ	SERIES/STAGE	AGE	SYSTEM			
WAPITI		WAPITI	BRAZEAU	MAASTRICHTIAN	66.4	UPPER	CRETACEOUS		
				CAMPANIAN	74.5				
PUSKWASKAU		COLORADO	WAPIABI	SANTONIAN	84.0				
BADHEART		BADHEART		CONIACIAN	87.5				
MUSKIKI		COLORADO	MUSKIKI	TURONIAN	88.5				
CARDIUM		CARDIUM	CARDIUM	CENOMANIAN	91.0				
KASKAPAU	KASKAPAU	COLORADO	OPABIN/VIMY		97.5	LOWER			
DUNVEGAN	DUNVEGAN	DUNVEGAN	DUNVEGAN	ALBIAN					
SHAFTESBURY		SHAFTESBURY	SHAFTESBURY						
BOULDER CR	CADOTTE	CADOTTE							
MULCROSS	HARMON	HARMON							
GATES	NOT/FALHER	NOT/FALHER	GATES						
MOOSEBAR	WILRICH	WILRICH	MOOSEBAR	APTIAN	113.0				
GETHING/CADOMIN	GETHING/CADOMIN	GETHING/CADOMIN	GLADSTON/CADOMIN	BARREMIAN	119.0				
				HAUTERIVIAN	124.0				
				VALANGINIAN	131.0				
MINNES	MINNES			BERRIASIAN	138.0				
				TITHONIAN	144.0	UPPER	JURASSIC		
FERNIE	FERNIE		NIKANASSIN	KIMMERIDGIAN	152.0				
			FERNIE	OXFORDIAN	156.0				
				CALLOVIAN	163.0	MIDDLE			
				BATHONIAN	169.0				
				BAJOCIAN	176.0	LOWER			
				AALENIAN	183.0				
			FERNIE	TOARCIAN	187.0				
FERNIE	FERNIE	FERNIE		PLIENSACHIAN	193.0	LOWER			
				SINEMURIAN	198.0				
			NORDEGG	HETTANGIAN	204.0				
					208.0				

Table 2. Synthesized stratigraphic correlation.  
 (D. Stott, personal communication, 1989)

The Stratigraphic Correlation chart of D. Stott (personal communication 1989) is the most recent update of stratigraphic correlation for the Western Canada Sedimentary Basin. The position of stratigraphic intervals within the stage boundary framework is based on biozone indicators. When the stratigraphic correlation chart is matched with the absolute time scale, the absolute age and severity of diachroneity can be estimated for each unit. For units that have boundaries other than stage boundaries, the absolute age was estimated by assuming equal intervals for substages, as described by Kauffman (1977) and Harland (1982). The equal intervals for substages are in turn based on equal intervals for biozones, as described above.

There are two sources of error when assigning absolute ages to unit boundaries. The first is the error associated with the age itself. For Cretaceous units, accuracy is variable depending on the method used for determination; it ranges from nearly zero to 2.5 Ma. The maximum error associated with Cretaceous stage boundaries is +/- 2.5 Ma for the Berriasian-Tithonian boundary (Palmer 1983). The error is likely enhanced when calculating formation boundary ages based on equal length biozones.

The error in absolute time introduces error in the accumulation rate which decreases with an increase in the time-span of the unit. For the units with durations greater than 1.1 Ma, error associated with the absolute age is comparably small and will not significantly affect the calculated accumulation rate. For the six units with durations of 1.1 Ma or less (Bluesky, Lower Kaskapau, Doe Creek, Cardium, Muskiki, and Badheart), error would not change the results of the study even if it is large, as these units occur in groups, and in times preceding or

following periods of rapid deformation. Based on the observed range in accumulation rates for other units (2000 - 224,000 kg/m<sup>2</sup>/Ma) there is a limit to the possible error associated with a unit's duration. The unit exists, and it is unreasonable to suggest that it was deposited in .1 Ma because the accumulation rate would be too high (order of magnitude) for a foreland basin setting. If the time duration of the unit can only have significant error in the positive direction, it must affect its neighbor in the negative direction, making the latter's sedimentation rate too high. In addition, the dimension of interest is the length of time represented by the deposition of a unit, obtained by subtracting the age of the unit's top from the age of the unit's base. This eliminates much of the error in the resultant time interval because a similar error is commonly associated with both the top and base. For example, if the age for the top and base of the Muskiki Formation are incorrect by +1.0 Ma each, the time interval for the unit remains constant and correct.

The second source of error is that associated with diachronous units, whose boundaries represent different ages in different portions of the study area. The only unit for which stratigraphic correlation shows noticeable discrepancies is the Fernie Group, within the Jurassic portion of the column. In the study area, the Fernie is not diachronous according to Stott's correlation (Table 2). However, in the Foothills near Brule, the Fernie Group represents about 8 Ma less than within the study area. This discrepancy is 13.7 % of the unit's maximum duration. Other units do not show significant diachroneity at the scale of the study. On this basis the mass accumulation rates are assumed to be unaffected by errors resulting from diachroneity.

The value assigned to a unit's duration is thus the best available estimate given the present state of knowledge of regional stratigraphic correlations and biostratigraphy in the basin. Error associated with the time duration of a unit translates into only minor error in the accumulation rate. The general trend in the magnitude of accumulation rates would not be significantly altered by error associated with absolute ages. The average accumulation rates fall into three distinct groups separated by large margins, and it would take an unusually large error in absolute age to move an accumulation rate from one group to another. In addition, the units which have short duration and could be most affected by dating errors occur on the flanks of major deformation intervals, where a shift between high and low accumulation rates would not seriously alter the overall pattern of deformation. For example, the Cardium has been assigned a duration of 0.6 Ma (Table 1). It has been estimated to be up to 2.8 Ma in duration based on other geological evidence, making a maximum possible error in duration of 2.2 Ma. As the neighboring Muskiki Formation is Coniacian, and the error on the Coniacian-Turonian boundary is only +/- 1.25 Ma, at least 1.0 Ma would have to be removed from the Upper Kaskapau Formation. The remaining 1.2 Ma can not be subtracted from the Muskiki or the Badheart, because they only represent 1.0 and 1.1 Ma each, and it would have to be removed from the Lower Puskwaskau Formation. The result of increasing the Cardium to 2.8 Ma would be to increase the accumulation rate of the Upper Kaskapau Formation, which is already in the high category, decrease the accumulation rate of the Cardium which already defines a period of quiescence, and increase the accumulation rate of the Lower Puskwaskau Formation from the base to the middle of

the moderate category. Thus, making this major alteration would only enhance the pattern already observed.



## 6. MASS ACCUMULATION RATES

The mass accumulation rate maps represent the rate of solid accumulation per unit area within a particular period of the basin's history. The averaged accumulation rates fall into three categories. The first is greater than  $148,000 \text{ kg/m}^2/\text{Ma}$ , the second is between  $73,000$  and  $115,000 \text{ kg/m}^2/\text{Ma}$ , and the third is less than  $35,000 \text{ kg/m}^2/\text{Ma}$ , referred to as high, medium, and low categories, respectively. Two main features can be read from mass accumulation rate maps which track activity in the basin and adjacent deformed belt at the time of deposition.

The first is the trend of contours, which reflects the provenance of sediment. The provenance, in turn, indicates the areas of the Cordillera which were actively deforming and eroding through time. The contours also depict the style of deposition, as being either from a point source such as a river, or a widespread shedding of sheets of sediment into the basin.

The second feature is the magnitude of the accumulation rate. The most likely cause of an increased sedimentation rate in the foreland basin, when a westerly source is indicated, is the generation of new relief in the deformed belt. High accumulation rate is taken to indicate rapid deformation in the deformed belt, and low accumulation rates to indicate periods of quiescence.

There may be a lag time between deformation and the resultant sedimentation. It is assumed that the lag is constant throughout deformation; therefore, accumulation rate mirrors the episodes of deformation in the adjoining Cordillera. The duration of deformation

events, or their magnitude as indicated by accumulation rate, is not affected by the lag time. As knowledge of the lag time for the Western Canadian foreland basin is not required, the accumulation rate history recorded in the foreland basin is simply correlated directly with deformation history in the Cordillera. In reality the deformation history must be shifted backwards on the absolute time scale by an undefined finite amount. Intuitively, the finite lag time is expected to be less than 0.5 Ma, as the accumulation rates have a resolution of that order. Deformation and erosion processes occur contemporaneously, supporting the notion of a short lag time. The influence of climate on erosion is assumed to remain constant during foreland basin development.

#### A. COMPARISON WITH ISOPACHS

Isopachs confirm the trends shown by mass accumulation rates and provide an independent estimate of the approximate source areas of sediment. The mass accumulation rate gives a more precise measure of the rate of accumulation, and of the location of source areas, because the effects of differential compaction are removed. More importantly, the mass accumulation rate reflects the intensity of deformation in the adjacent Cordillera because it includes a time component. Figures 6a and 6b show the differences between the isopach and the mass accumulation rate of the Harmon Formation. The fan of high accumulation, which indicates an easterly source region, is not as distinct from the isopach. If only the isopach was considered, the source may be interpreted as Cordilleran. Also, the magnitude of

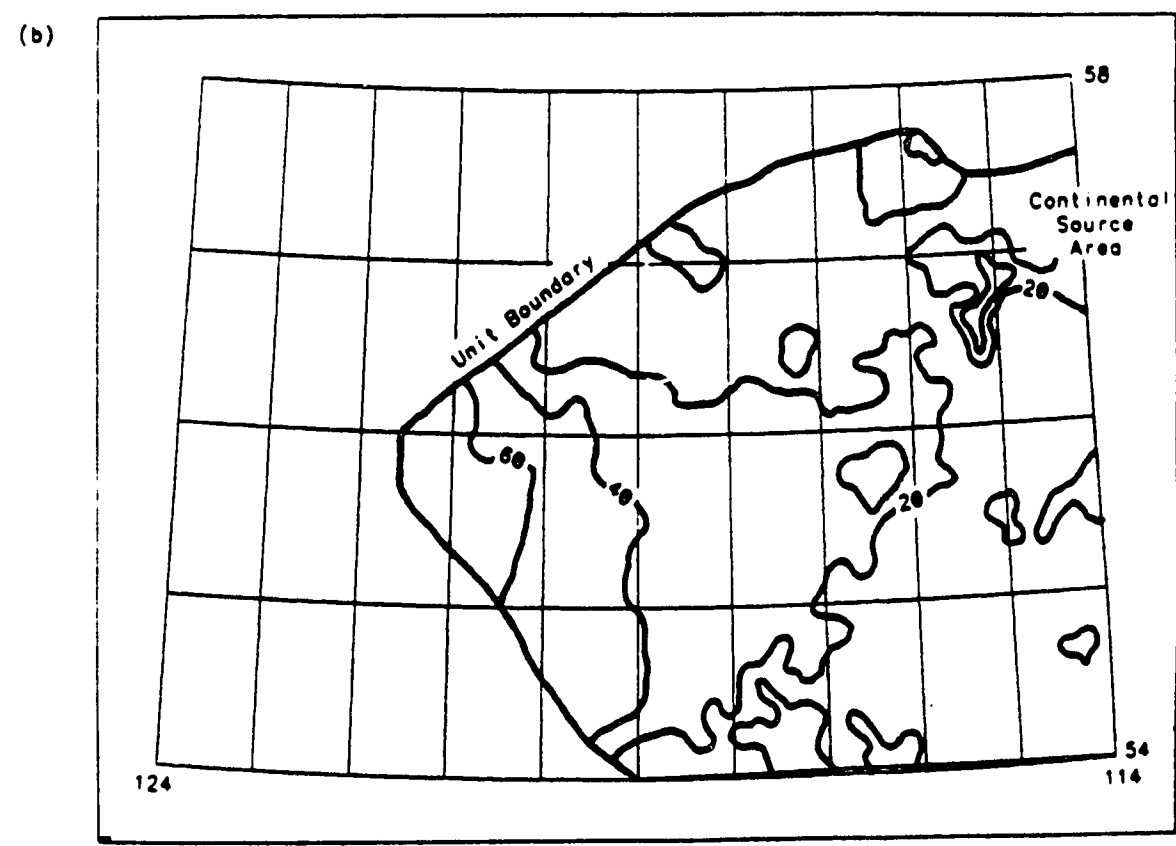
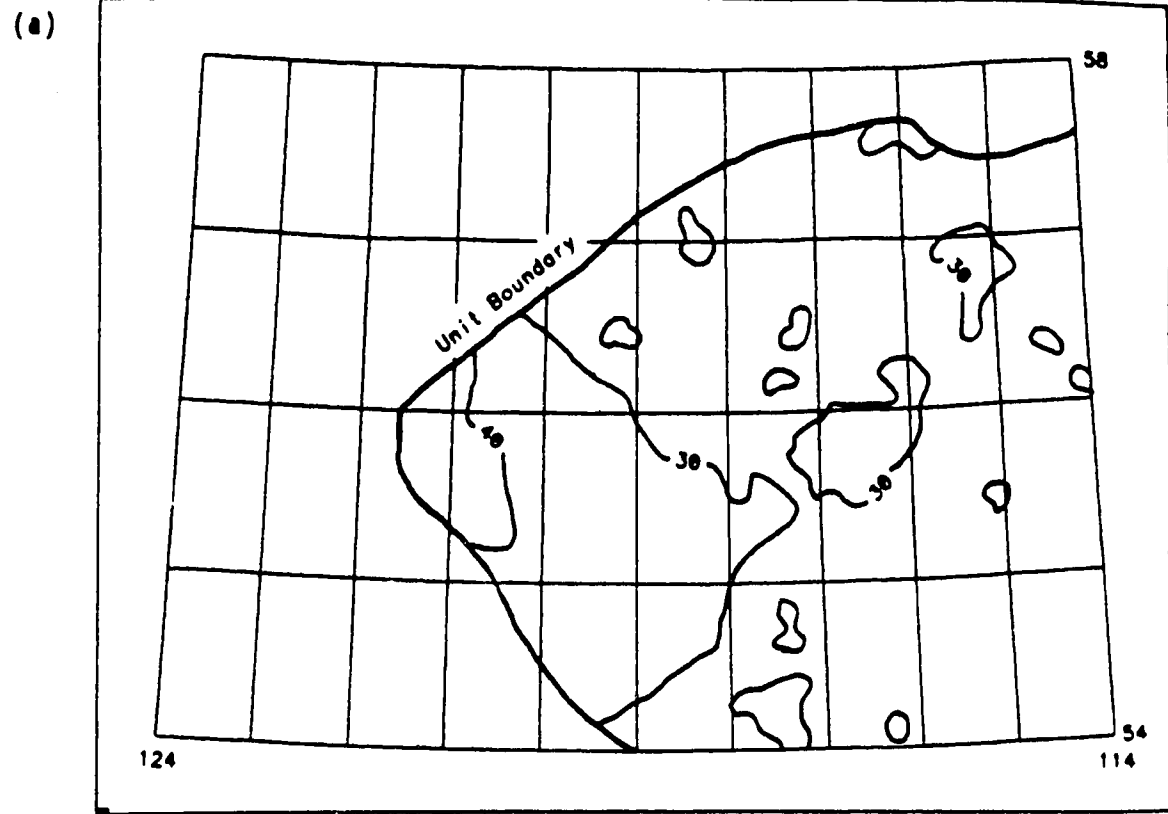


Figure 6. Lower Peace River Group. (a) Isopach (m);  
(b) Mass accumulation rate ( $\text{kg}/\text{m}^2/\text{Ma} \times 10^3$ ).

accumulation is low when compared to other foreland basin units. This information is not conveyed by isopachs alone.

## 7. INTERPRETATIONS

Mass accumulation rate maps have two attributes related to conditions of the basin and adjacent deformed belt at the time of deposition. Firstly, the distribution of accumulation rates for any particular unit indicates both the broad environment of deposition and the provenance of the sediment. Secondly, the magnitude of the mass accumulation rate indicates the severity of the deformation giving rise to the unit's deposition.

### A. FERNIE GROUP

The Fernie Group has a low average mass accumulation rate ( $2 \times 10^3 \text{ kg/m}^2/\text{Ma}$ ). This low rate is an artifact of extensive erosion. Deposition of the Fernie Group marks the beginning of foreland basin development. For the Fernie Group to represent rapid accumulation with rates in the order of  $200 \times 10^3 \text{ kg/m}^2/\text{Ma}$ , the isopach would have to be two orders of magnitude thicker than observed. This would suggest an original thickness of the order of 20 km rather than the observed 200 m. As such a thickness is unlikely, and as high elevation is not expected in the initial stages of deformation (cf. Stockmal and Beaumont, 1987), it is assumed that the Fernie Group likely records moderate to low mass accumulation. Hall (1984) suggested that the Fernie Group may not be extensively eroded. This supports the accommodation of initial deformation largely below sea level, resulting in low rates of sediment accumulation.

The Fernie is regionally diachronous, representing a shorter

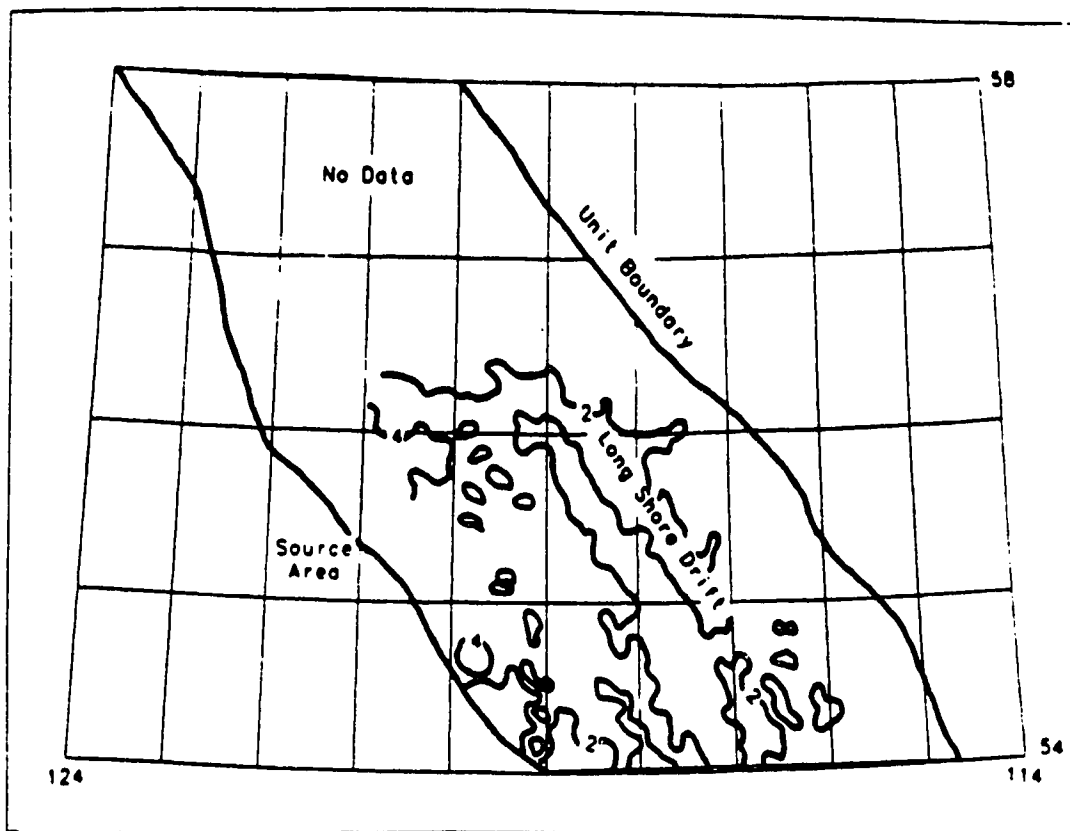
time interval to the south of the study area but diachroneity is not a serious problem at the scale of the study area, especially when compared to the large time interval the unit represents (see above). A single value of 58.4 Ma was used as the duration of the Fernie within the study area.

Mass accumulation rate contours for the Fernie Group are parallel to the strike of the deformed belt, showing that initial deformation occurred across the study area, with a concentration between 54° and 57°N (Figure 7a). Deformation resulted in sediment being shed northeastward into the basin, accumulating in a southwesterly thickening wedge. The stringer of higher accumulation rates parallel to the deformed belt farther to the northeast indicates that longshore drift contributed to the redistribution of sediment. The northwest end of the stringer is connected to the zone of higher accumulation along the thrust-fold belt, suggesting that current flowed to the southeast.

#### B. BULLHEAD GROUP

The Bullhead Group was deposited over 6 Ma, with a low average mass accumulation rate ( $24 \times 10^3 \text{ kg/m}^2/\text{Ma}$ ). At this early stage of orogenesis, most of the deformation was still being accommodated on the edge of the craton below sea level, producing little relief to induce higher erosion. The distribution of contours has a pattern similar to the Fernie Group. The source region was between 54° and 57°N, and sediments were shed in sheets to the northeast (Figure 7b), and collected in a narrow trough running parallel to the Cordillera. Most of the region to the northeast received very little sediment and was

(a)



(b)

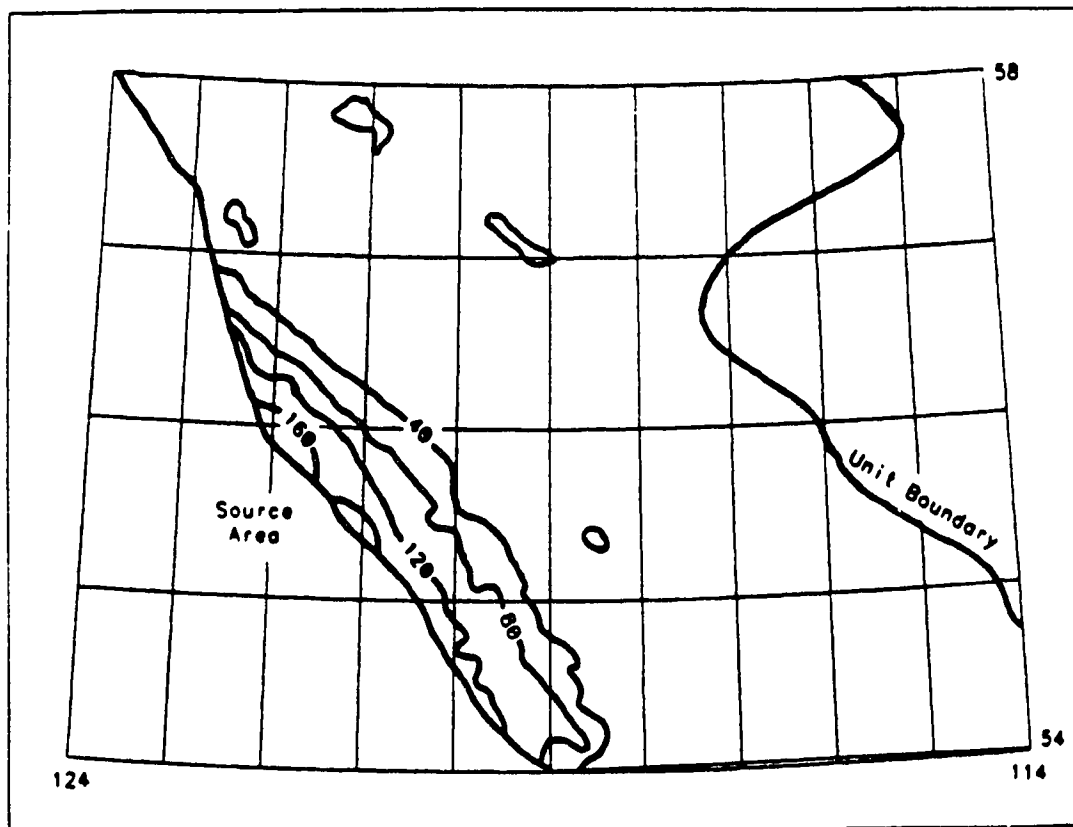


Figure 7. Mass accumulation rate ( $\text{kg/m}^2/\text{Ma} \times 10^3$ ). (a) Fernie Group; (b) Bullhead Group.

likely dominated by easterly sources.

### C. BLUESKY FORMATION

The Bluesky Formation spans 0.8 Ma, and marks the first major pulse of rapid sediment accumulation ( $185 \times 10^3 \text{ kg/m}^2/\text{Ma}$ ). The distribution of contours describes a broader basin than for the Bullhead, with the source remaining in a similar location, between  $54^\circ$  and  $57^\circ\text{N}$ . Sediments were shed northeast in sheets across the basin into a southwesterly thickening wedge (Figure 8a).

### D. LOWER SPIRIT RIVER GROUP

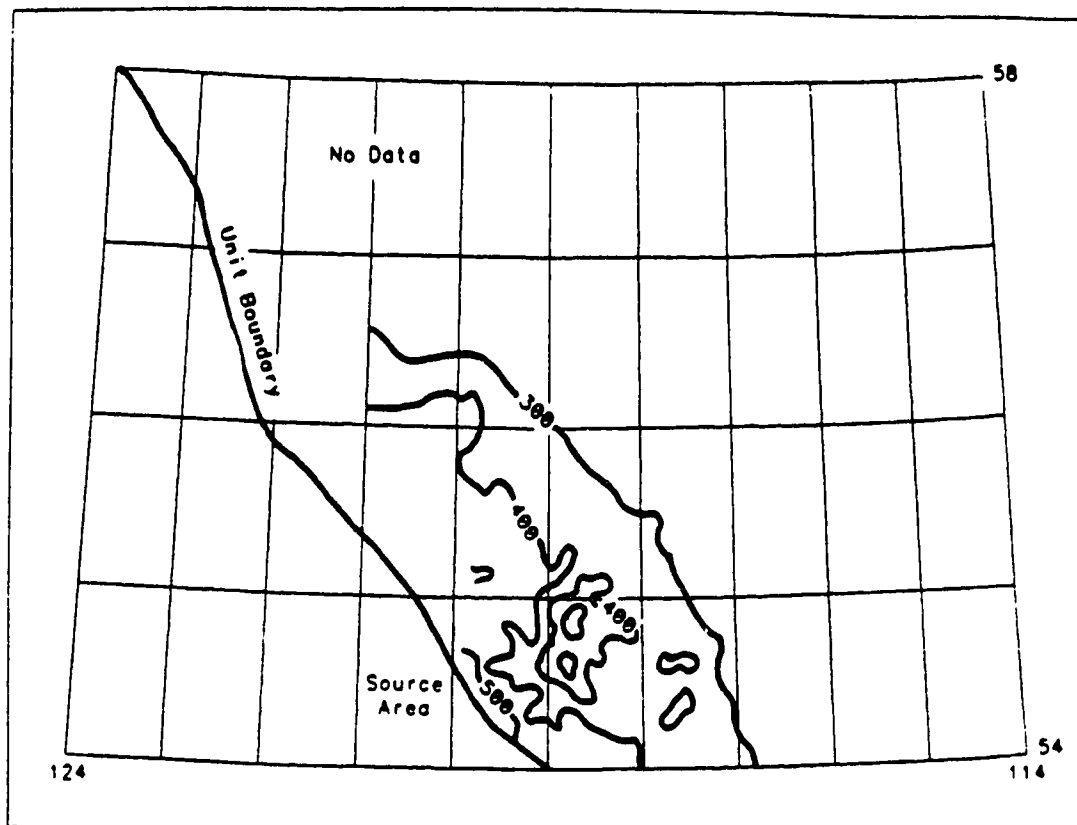
The Lower Spirit River Group represents deposition during a 1.8 Ma interval and records a lower average rate of accumulation ( $98 \times 10^3 \text{ kg/m}^2/\text{Ma}$ ) than the Bluesky unit. Lower Spirit River time was a period of quiescence in the Cordillera. The pattern of accumulation rate contours is generally indistinct; however, there is a clear northwesterly shift in the zone of highest accumulation to a localized source near  $56^\circ\text{N}$  (Figure 8b) when compared to the Bluesky Formation. There is no longer parallelism with the deformed belt, but rather an arcuate pattern around the northwest area of maximum accumulation.

### E. UPPER SPIRIT RIVER GROUP

The Upper Spirit River Group spans 2.3 Ma, and marks a second pulse of rapid deformation resulting in a high average accumulation



(a)



(b)

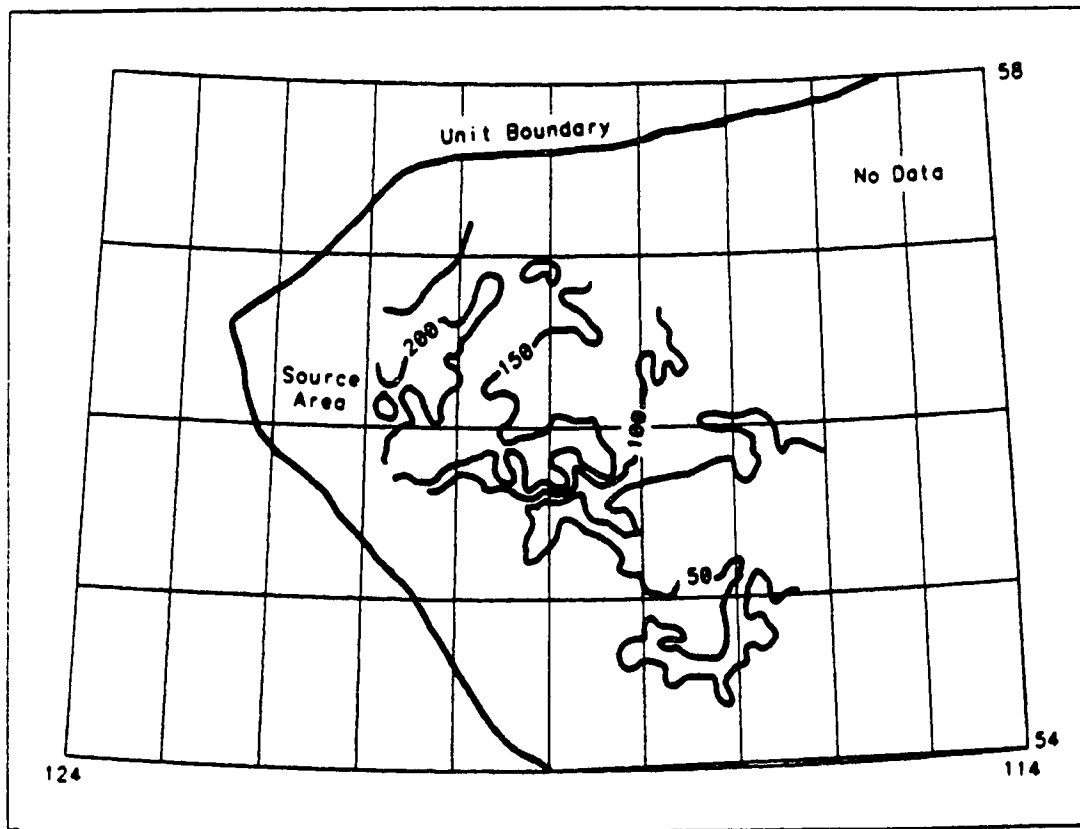


Figure 8. Mass accumulation rate ( $\text{kg/m}^2/\text{Ma} \times 10^3$ ). (a) Bluesky Formation; (b) Lower Spirit River Group.

rate ( $224 \times 10^3 \text{ kg/m}^2/\text{Ma}$ ) in the basin. The source was localized between  $54^\circ$  and  $56^\circ\text{N}$ , with accumulation contours fanning around the source region (Figure 9a). This unit shows characteristics similar to the Lower Spirit River, but with the source region being larger, more southerly located, and with a higher intensity of deposition.

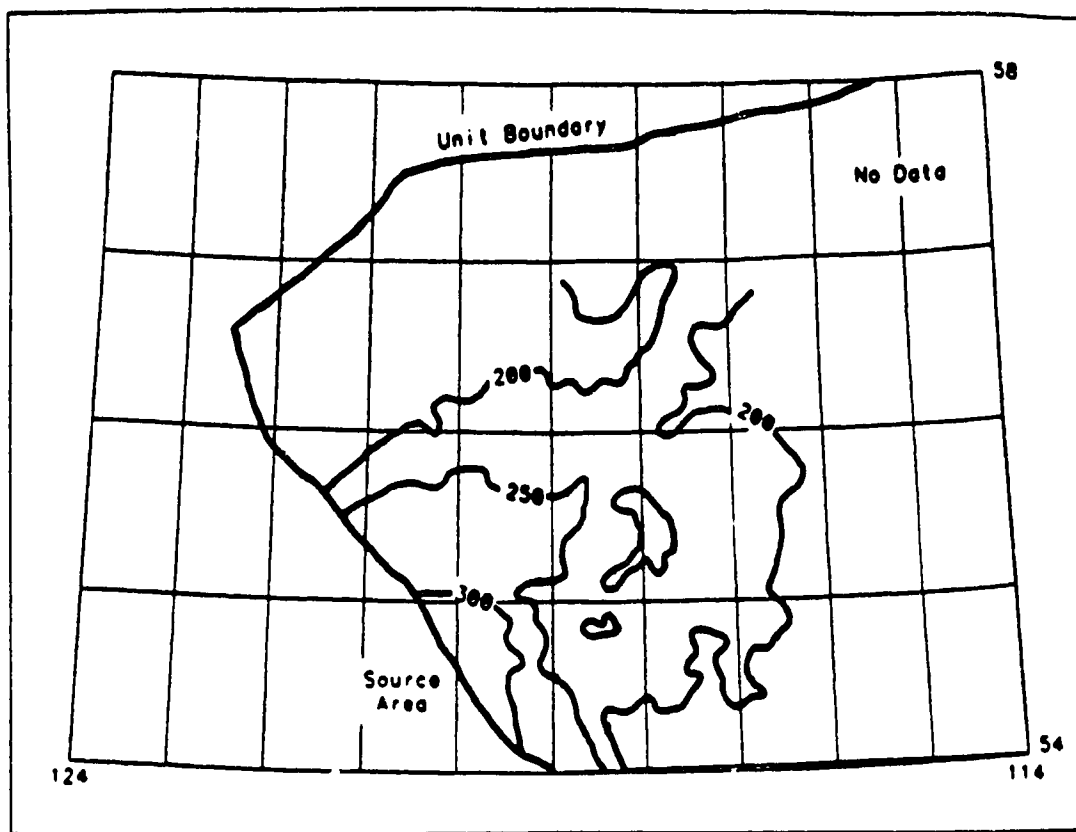
#### F. LOWER PEACE RIVER GROUP

The Lower Peace River Group represents a 1.7 Ma interval and marks a return to quiescence, with a low average rate of accumulation in the basin ( $24 \times 10^3 \text{ kg/m}^2/\text{Ma}$ ). There is a weak localized Cordilleran source at  $56^\circ\text{N}$  (Figure 9b). This source region had a limited influence on the accumulation rate distribution. Easterly derived sediment dominates the accumulation rate distribution, with a source between  $56^\circ$  and  $57^\circ\text{N}$  in the east. A fan of higher accumulation rate contours spread out westward across the basin.

#### G. UPPER PEACE RIVER GROUP

The Upper Peace River Group spans 1.7 Ma and represents continued quiescence in the deformed belt, with an average accumulation rate ( $34 \times 10^3 \text{ kg/m}^2/\text{Ma}$ ) only slightly higher than the underlying Lower Peace River Group. The local Cordilleran source is beginning to overprint the contour pattern associated with the easterly source outlined by the Lower Peace River unit. Also, the Cordilleran source region moved slightly south to a location between  $55^\circ$  and  $56^\circ\text{N}$  (Figure 10a). The easterly source is still distinguishable, as it supplied most of the

(a)



(b)

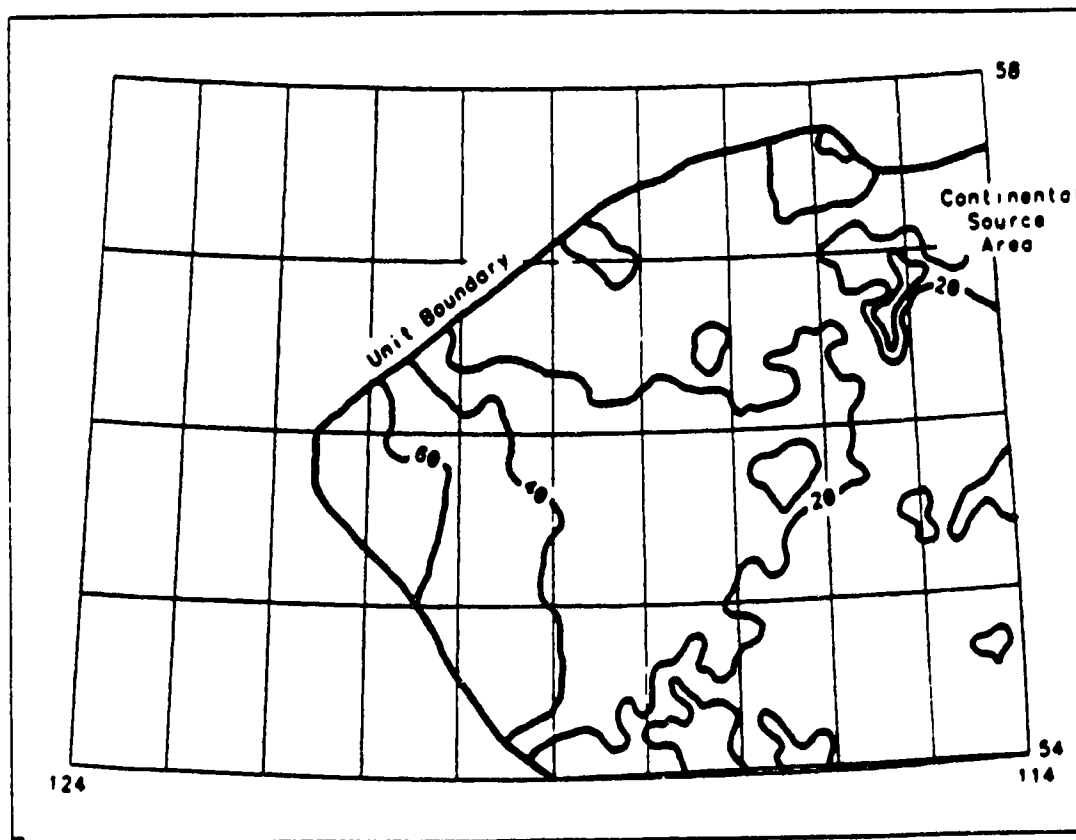
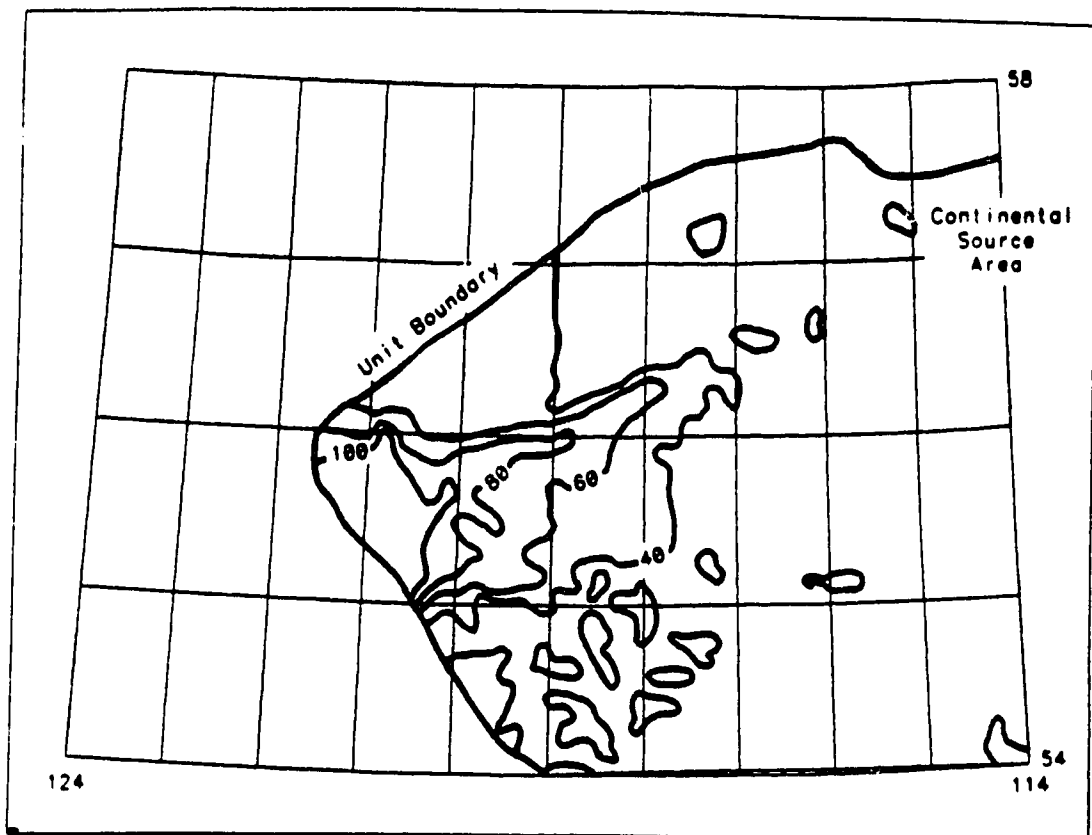


Figure 9. Mass accumulation rate ( $\text{kg/m}^2/\text{Ma} \times 10^3$ ). (a) Upper Spirit River Group; (b) Lower Peace River Group.

(a)



(b)

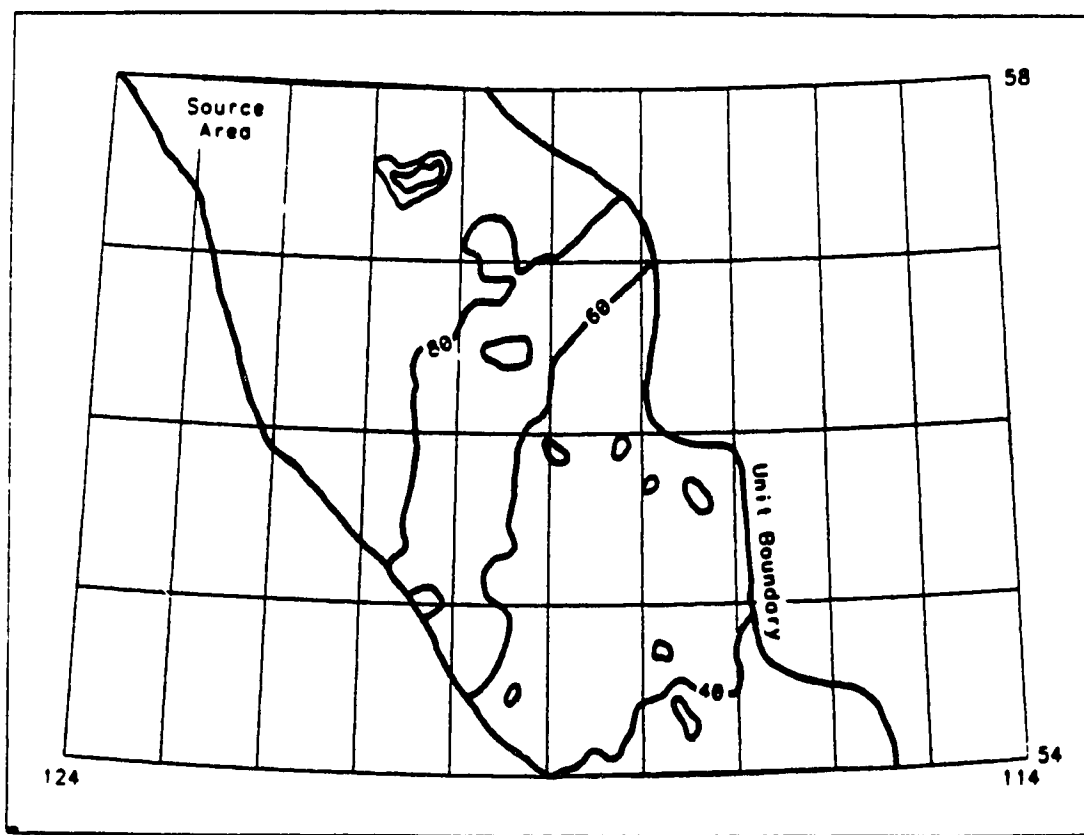


Figure 10. Mass accumulation rate ( $\text{kg/m}^2/\text{Ma} \times 10^3$ ). (a) Upper Peace River Group; (b) Shaftesbury Formation.

sediment for at least the eastern half of the unit. This agrees with existing interpretations that much of the Upper Peace River unit is continentally derived, based on other geological data (D. Leckie personal communication 1989).

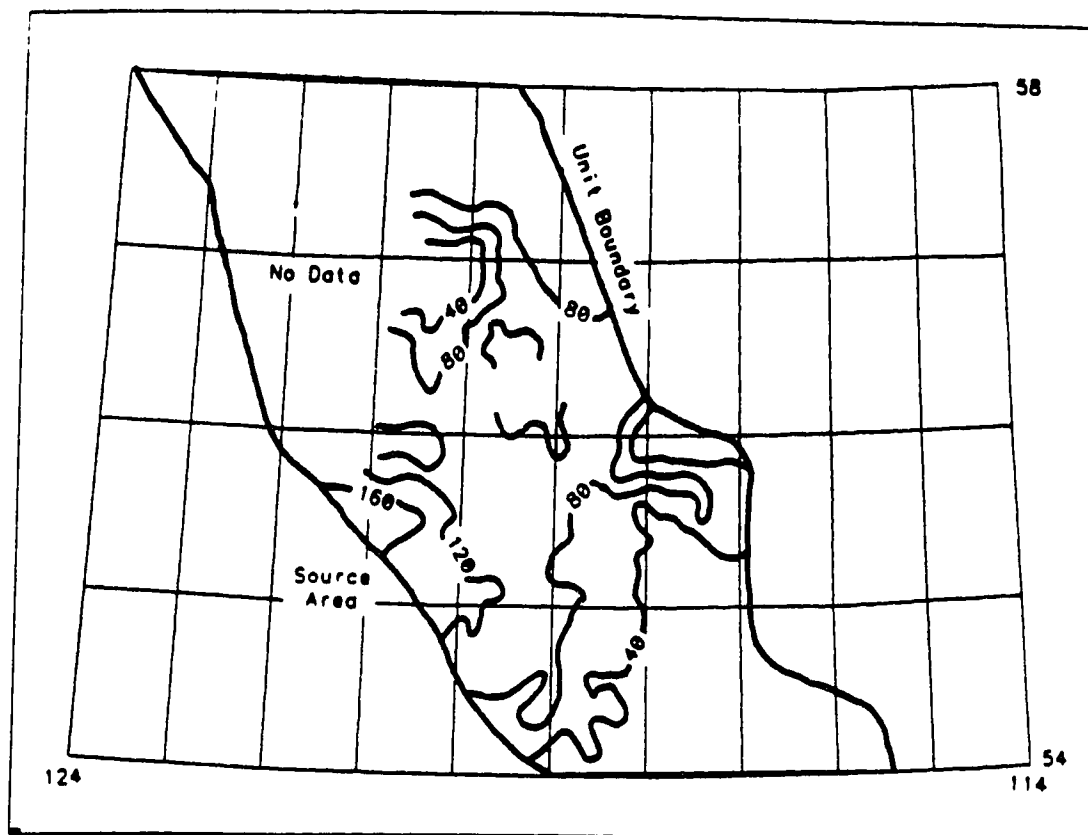
#### H. SHAFTESBURY FORMATION

The Shaftesbury Formation represents a 7.8 Ma interval and marks an increase to a moderate rate of accumulation ( $106 \times 10^3 \text{ kg/m}^2/\text{Ma}$ ). When compared to the Upper Peace River unit, it shows a dramatic northward shift in the Cordilleran source region to a position north of  $57^\circ\text{N}$  (Figure 10b). This northerly source significantly changes the pattern of the accumulation contours to a northeast-southwest orientation. Sediment from the deformed belt are shed in sheets accumulating in a southeasterly tapering wedge, nearly normal to previous trends.

#### I. DUNVEGAN FORMATION

The Dunvegan Formation spans 2.5 Ma, and represents continued moderate average accumulation ( $89 \times 10^3 \text{ kg/m}^2/\text{Ma}$ ), indicating only moderate deformation. The main source area migrated southward and became more localized. The source area was situated between  $55^\circ$  and  $56^\circ\text{N}$ , with additional minor sources farther north (Figure 11a). The contour distribution is mostly indistinct, with a rough arc about the west central source area.

(a)



(b)

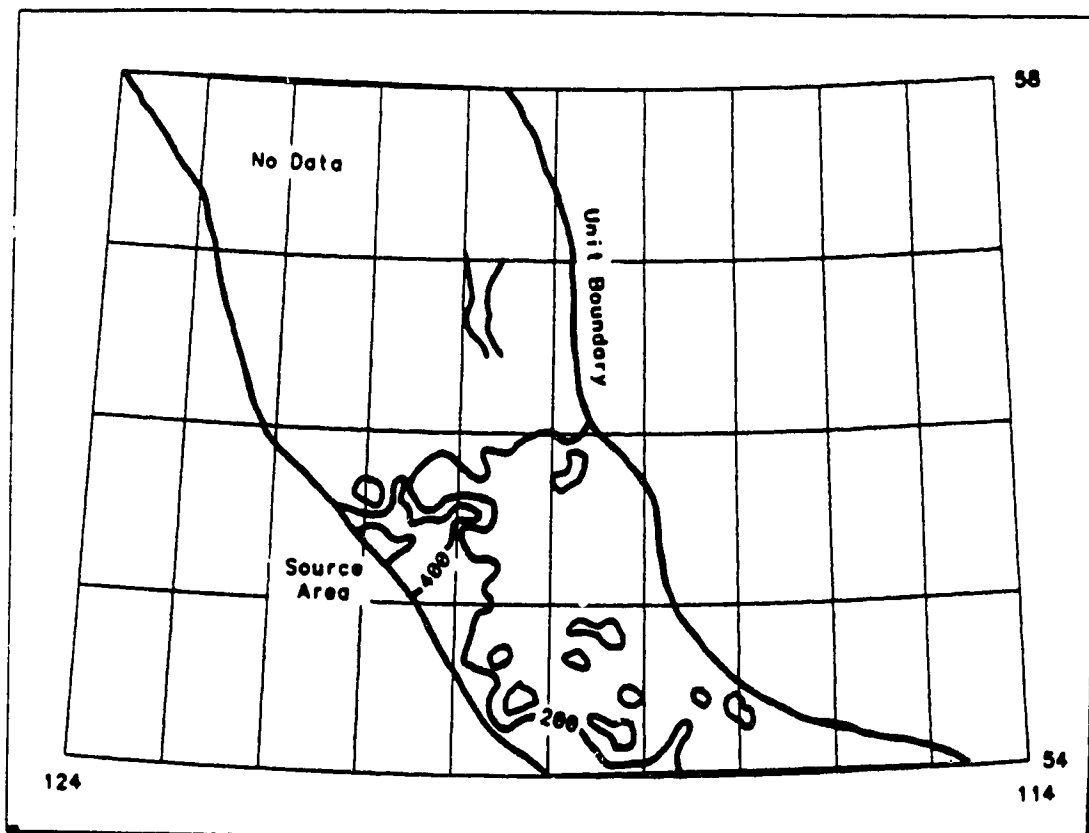


Figure 11. Mass accumulation rate ( $\text{kg/m}^2/\text{Ma} \times 10^3$ ). (a) Dunvegan Formation; (b) Lower Kaskapau Formation.

## J. LOWER KASKAPAU FORMATION

The Lower Kaskapau Formation spans 0.5 Ma and records a pulse of rapid deformation. The high rate of mass accumulation ( $186 \times 10^3 \text{ kg/m}^2/\text{Ma}$ ) indicates that rapid deformation was initiated during this time. The contours suggest that several localized areas gave rise to the high accumulation rates in the basin (Figure 11b). The main source is located between  $55^\circ$  and  $56^\circ\text{N}$ , with additional sources at  $54^\circ$  and  $57^\circ\text{N}$ . Each source has a fan of sediment centered on it.

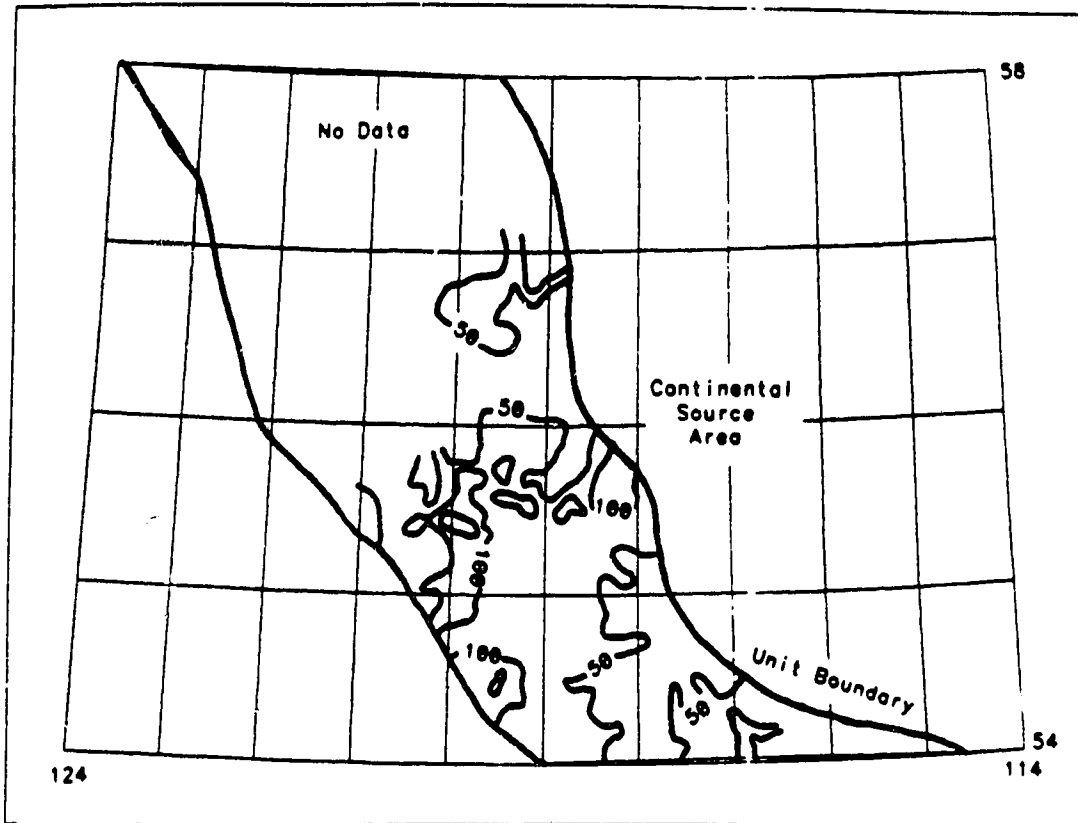
## K. DOE CREEK FORMATION

The Doe Creek Formation covers 0.4 Ma, and represents a pause in deformation, with a moderate accumulation rate ( $94 \times 10^3 \text{ kg/m}^2/\text{Ma}$ ), and no obvious Cordilleran source (Figure 12a). A deltaic fluvial system extended from the craton to the east between  $55^\circ$  and  $56^\circ\text{N}$ . The Cordillera continued to shed minor volumes of sediment into the basin from the west, but sedimentation from the east was dominant.

## L. UPPER KASKAPAU FORMATION

The Upper Kaskapau Formation spans 4.4 Ma, and represents another pulse of rapid accumulation ( $210 \times 10^3 \text{ kg/m}^2/\text{Ma}$ ). Deformation had spread out to encompass the entire western edge of the units extent, with a strong accumulation contour pattern parallel to the strike of the thrust-fold belt (Figure 12b). Sediments from the deformed belt were

(a)



(b)

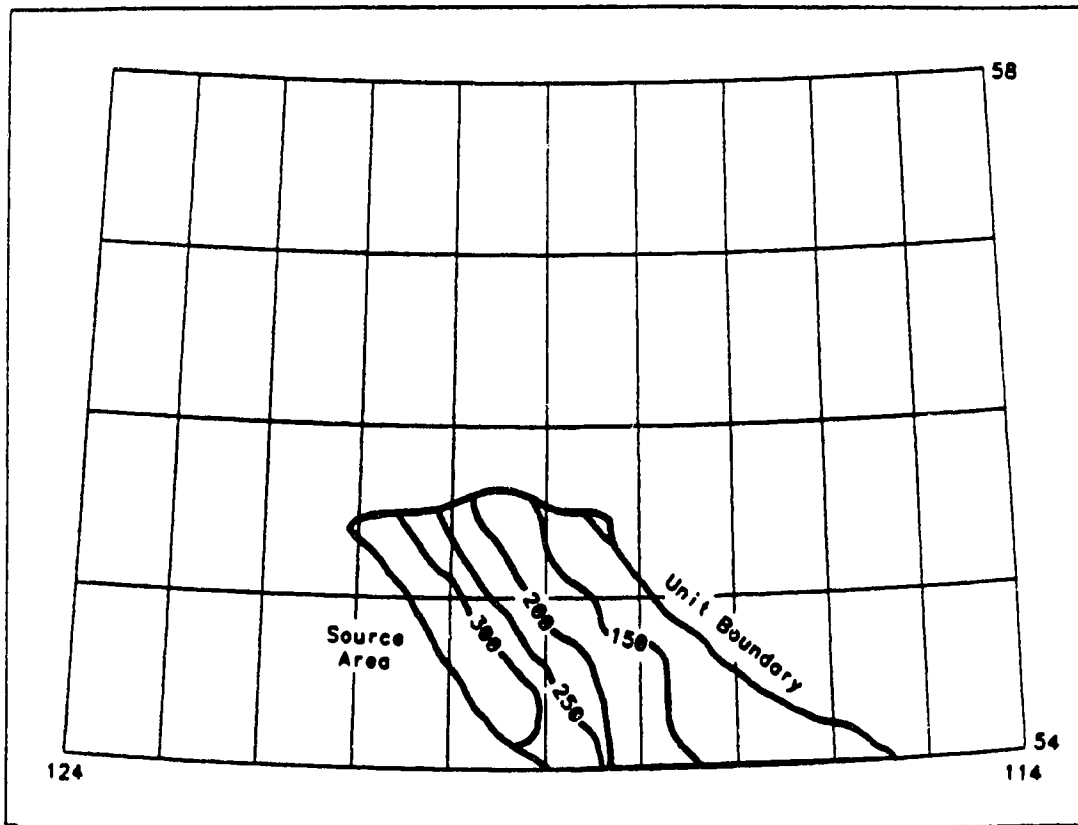


Figure 12. Mass accumulation rate ( $\text{kg/m}^2/\text{Ma} \times 10^3$ ). (a) Doe Creek Formation; (b) Upper Kaskapau Formation.



shed in sheets eastward into a westerly thickening wedge.

#### M. CARDIUM FORMATION

The Cardium Formation represents a 0.6 Ma interval and records an average accumulation rate of moderate magnitude ( $93 \times 10^3 \text{ kg/m}^2/\text{Ma}$ ), marking a lull in the rapid deformation. The pattern of accumulation contours is similar to that of the Upper Kaskapau, only more subdued. The source area in the Cordillera is more pronounced in the southwest; however, sediment continued to be shed from the Cordillera along the length of the unit (Figure 13a).

#### N. MUSKIKI FORMATION

The Muskiki Formation spans 1.0 Ma and was the result of a pulse of rapid accumulation ( $149 \times 10^3 \text{ kg/m}^2/\text{Ma}$ ) during rapid deformation. A source region predominantly in the south caused contours to trend northwest-southeast (Figure 13b). Sediments from the deformed belt were shed as sheets in a northeasterly tapering wedge.

#### O. BADHEART FORMATION

The Badheart Formation represents a 1.1 Ma interval and marks a return to low average accumulation ( $27 \times 10^3 \text{ kg/m}^2/\text{Ma}$ ) and a period of quiescence in the Cordillera after major deformation. The Badheart Formation is characterized by low rates of accumulation and the distribution of accumulation contours indicates a localized Cordilleran

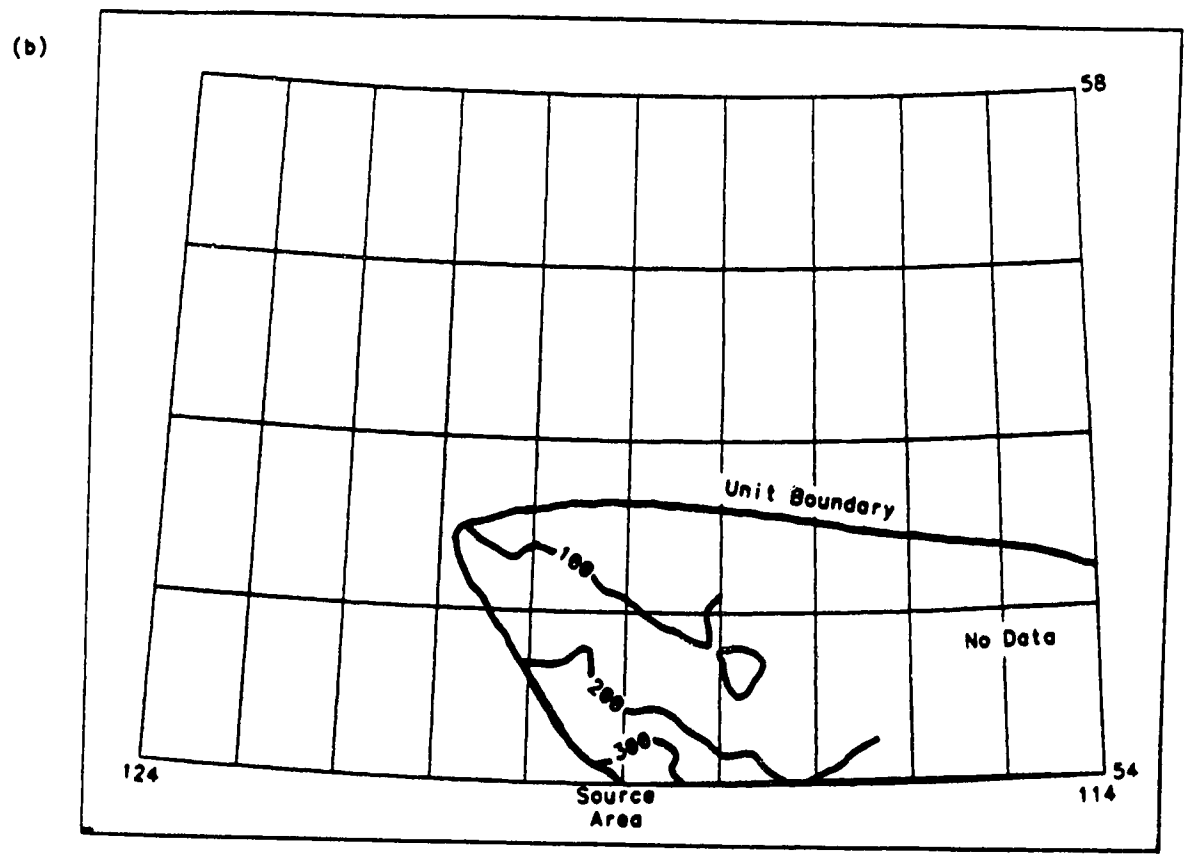
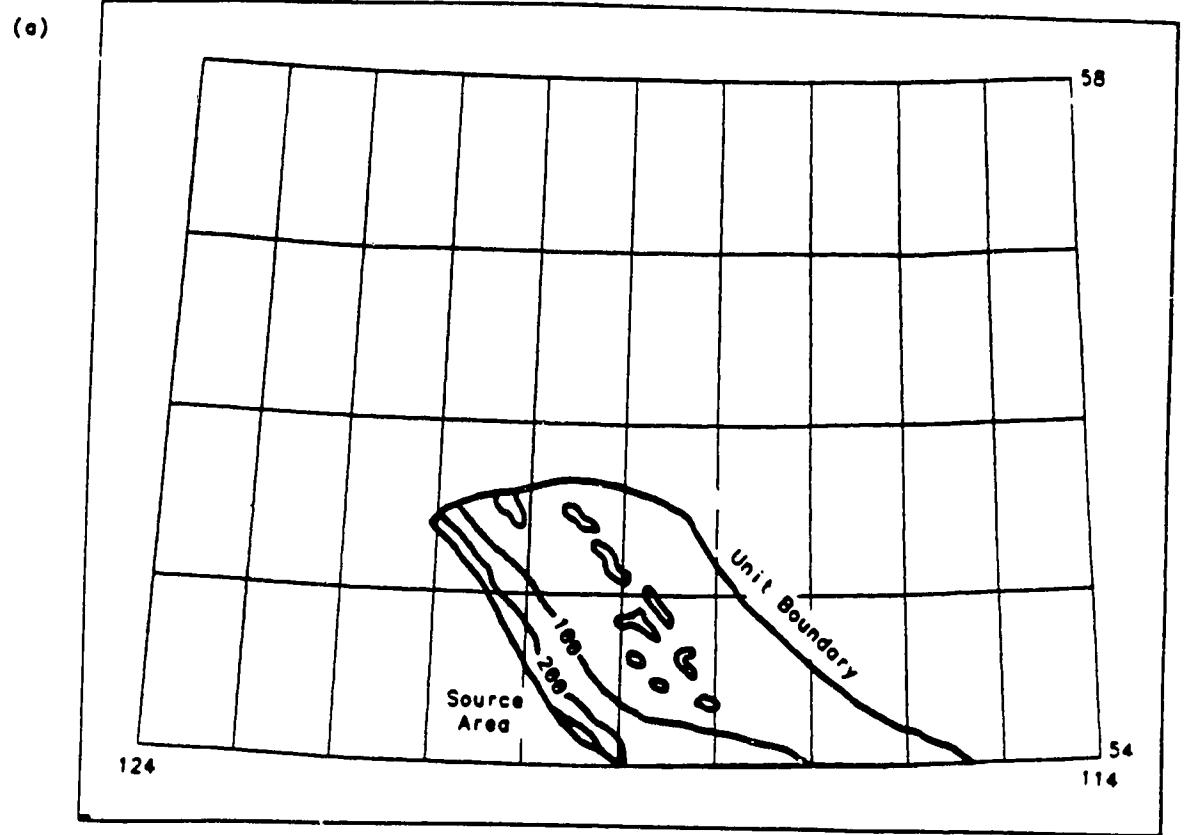


Figure 13. Mass accumulation rate ( $\text{kg/m}^2/\text{Ma} \times 10^3$ ). (a) Cardium Formation; (b) Muskiki Formation.

source between 54° and 55°N with sediment fanning out into the basin from the source (Figure 14a).

#### P. LOWER PUSKWASKAU FORMATION

The Lower Puskawaskau Formation represents a 5.1 Ma interval and is characterized by a moderate average accumulation rate ( $74 \times 10^3 \text{ kg/m}^2/\text{Ma}$ ). The source region was in the south with a pattern similar to the Muskiki Formation. Sediments from the deformed belt were shed northeastward in a southwesterly thickening wedge (Figure 14b).

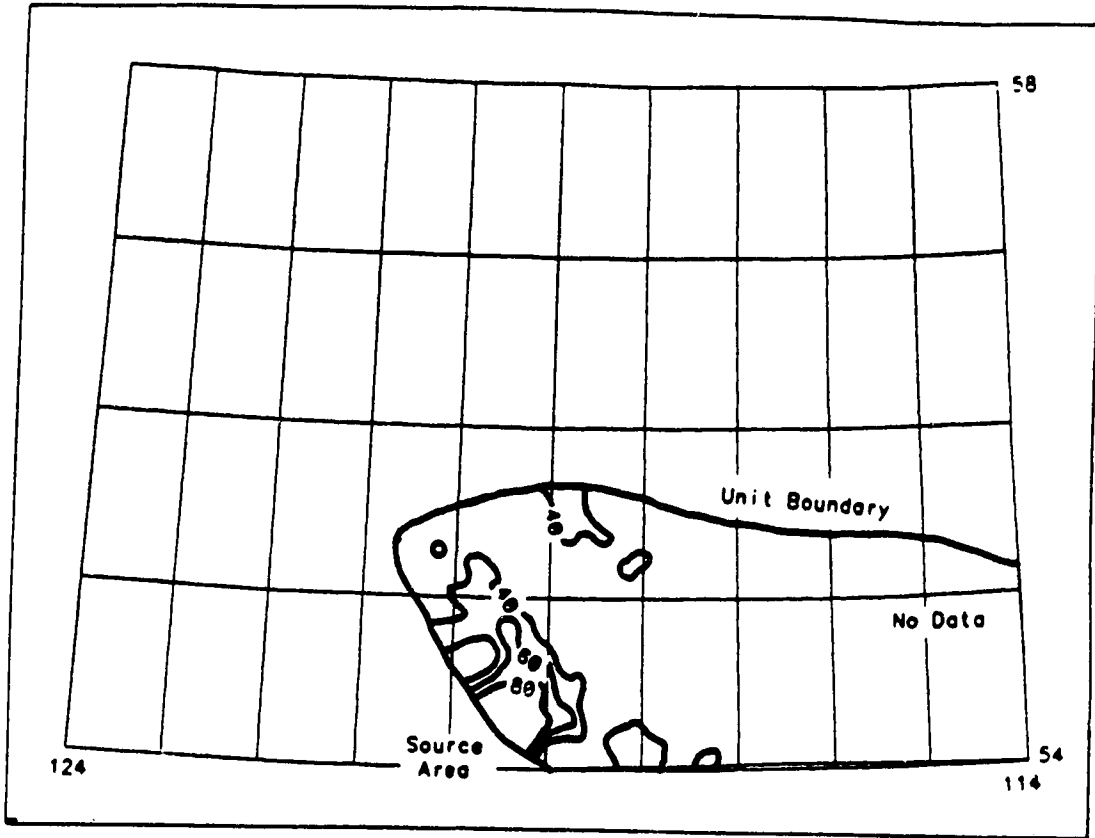
#### Q. CHINOOK FORMATION

The Chinook Formation spans 1.3 Ma, and shows a low average accumulation rate ( $15 \times 10^3 \text{ kg/m}^2/\text{Ma}$ ) with a northward shift in the source region compared to the Lower Puskawaskau Formation. The accumulation contours indicate a localized source at 55°N, and another minor source in the southwest which is likely a remnant of the source region of the Lower Puskawaskau Formation. Sediment accumulated in an easterly tapering wedge, with accumulation contours trending north south (Figure 15a).

#### R. UPPER PUSKWASKAU FORMATION

The Upper Puskawaskau Formation spans 1.3 Ma and is the uppermost unit which can be quantified confidently in terms of accumulation

(a)



(b)

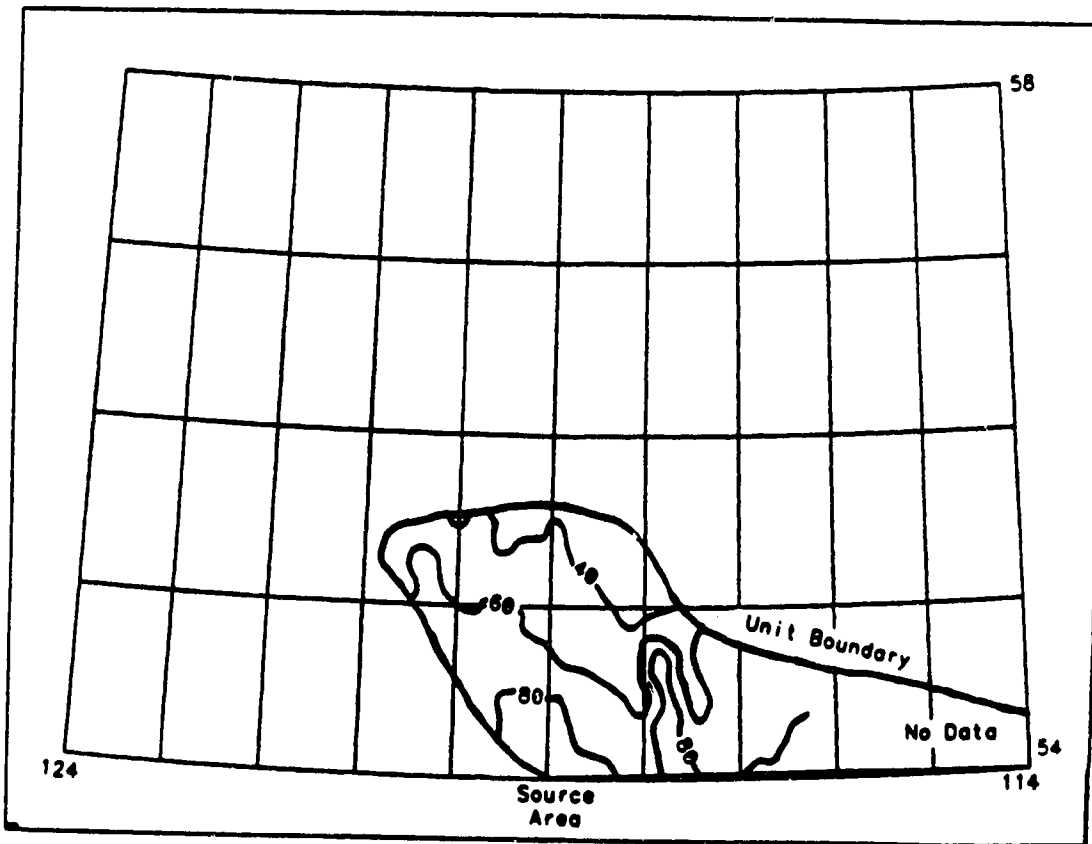
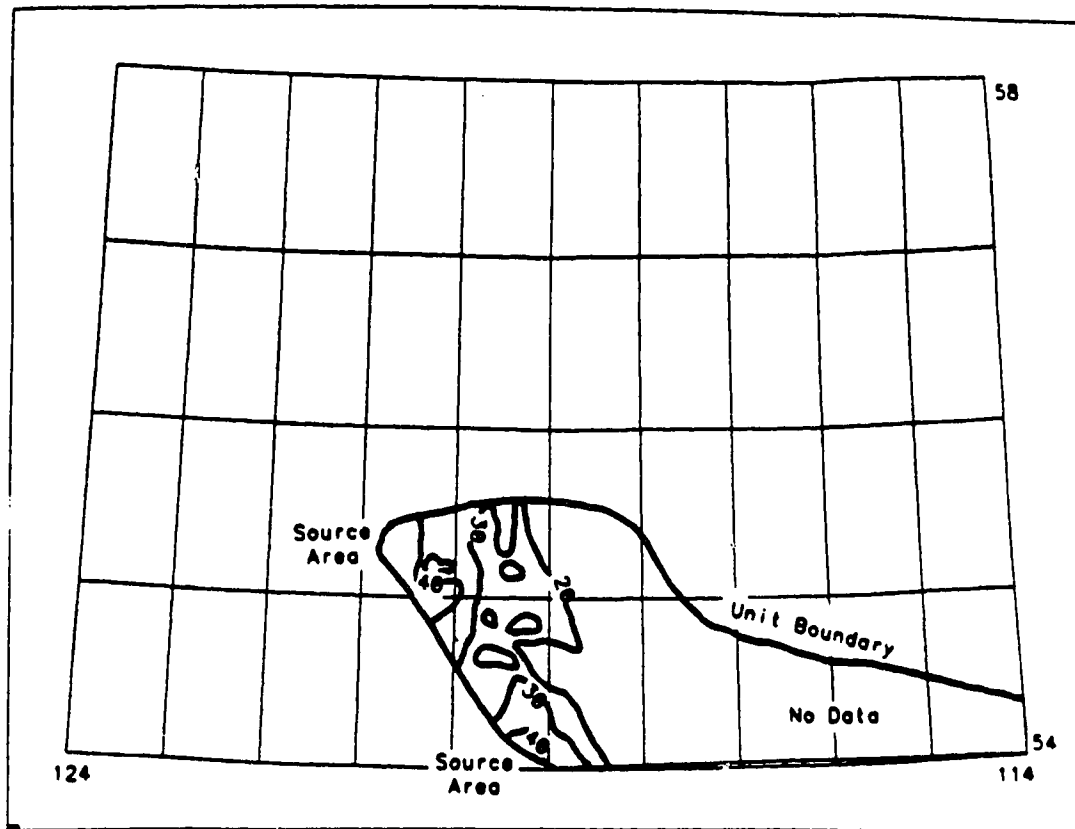


Figure 14. Mass accumulation rate ( $\text{kg}/\text{m}^2/\text{Ma} \times 10^3$ ). (a) Badheart Formation; (b) Lower Puskwaskau Formation.

(a)



(b)

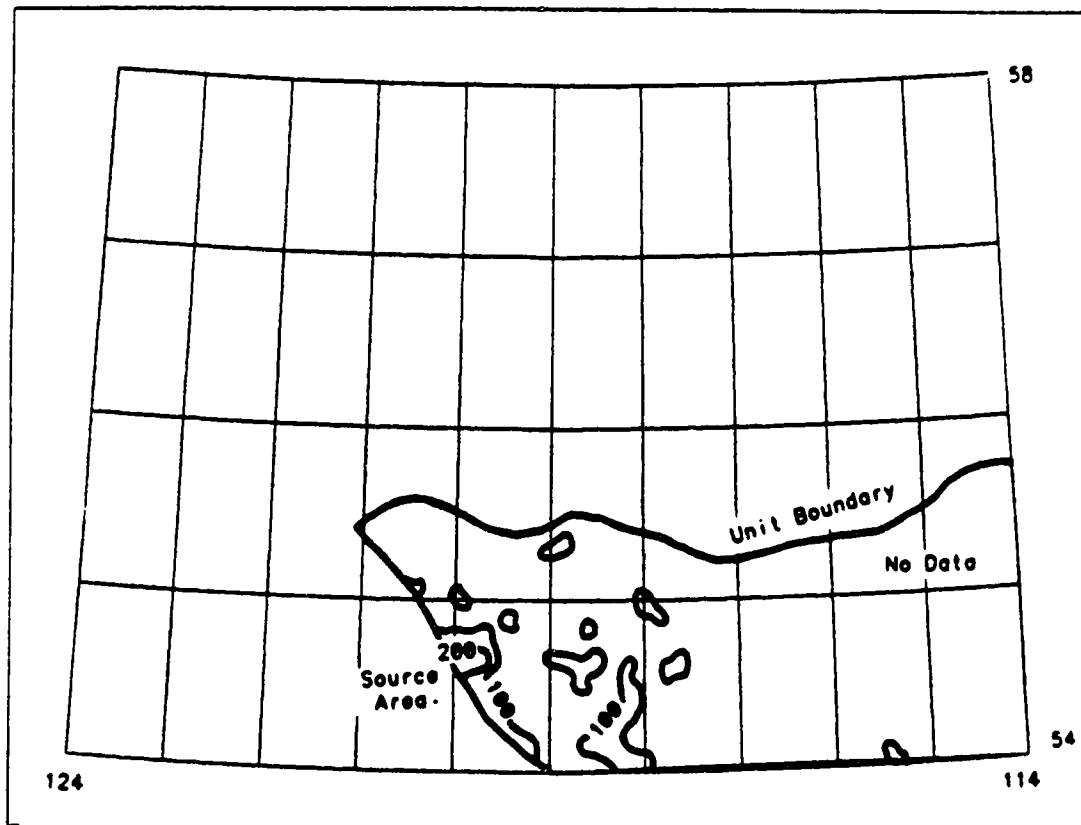


Figure 15. Mass accumulation rate ( $\text{kg/m}^2/\text{Ma} \times 10^3$ ). (a) Chinook Formation; (b) Upper Puskwaskau Formation.

rates. It shows a moderate average accumulation rate  
( $116 \times 10^3 \text{ kg/m}^2/\text{Ma}$ ), with a localized point source between  $54^\circ$  and  $55^\circ\text{N}$   
(Figure 15b).

## 8. DISCUSSION

During foreland basin development, the Canadian Cordillera deformed through the docking and accretion of foreign terranes at the outboard edge of the continental margin (Monger 1984). This convergent deformation loaded the craton, causing a downward flexure, and provided a western sedimentary source to fill the foreland basin. The distribution and magnitude of mass accumulation rates for specific units can be linked to deformation within the Cordillera. Both the location and magnitude of deformation can be estimated through time by examining the average rate of accumulation and the provenance of sediment for specific units within the foreland basin.

### A. CYCLIC NATURE OF DEFORMATION

If the average accumulation rates for each unit are plotted against time, a cyclic pattern of accumulation emerges. Figure 16 shows two groups of rapid accumulation, each defining a rapid deformation episode in the Cordillera; the first lasts from 108 to 113 MaBP and the second lasts from 87 to 94 MaBP. Prior to early Aptian and after late Campanian time the stratigraphic column contains major unconformities, making the mass accumulation rate difficult to quantify, and outside the range under consideration.

There are two-and-a-half deformation cycles defined in Figure 16. The first cycle begins in the Aptian with the deposition of the Bullhead Group resulting from low deformation. Rapid deformation then

UNIT	AGE RANGE (Ma)	DURATION (Ma)	RANGE OF ACCUMULATION RATE ( $10^3 \text{ kg/m}^2/\text{Ma}$ )	AVE. ACCUMULATION RATE ( $10^3 \text{ kg/m}^2/\text{Ma}$ )
U Puskwaskau	77.5 - 78.8	1.3	2 - 408	116
Chinook	78.8 - 81.3	2.5	0 - 52	15
L Puskwaskau	81.3 - 86.4	5.1	0 - 120	74
Badheart	86.4 - 87.5	1.1	2 - 142	27
Muskiki	87.5 - 88.5	1.0	2 - 459	149
Cardium	88.5 - 89.1	0.6	4 - 587	93
U Kaskapau	89.1 - 93.5	4.4	92 - 352	210
Doe Creek Top	93.5 - 93.9	0.4	4 - 776	94
L Kaskapau	93.9 - 94.4	0.5	4 - 341	186
Dunvegan	94.4 - 96.9	2.5	1 - 320	89
Shaftesbury	96.9 - 104.7	7.8	11 - 394	106
U Peace River	104.7 - 106.4	1.7	4 - 152	34
L Peace River	106.4 - 108.1	1.7	7 - 116	24
U Spirit River	108.1 - 110.4	2.3	0 - 440	224
L Spirit River	110.4 - 112.2	1.8	0 - 321	98
Bluesky	112.2 - 113.0	0.8	4 - 1,570	185
Bullhead	113.0 - 119.0	6.0	0 - 270	24
Fernie	141.6 - 200.0	58.4	0 - 9	2

Table 3. Absolute age and mass accumulation rate data for all units.

### Accumulation Rate versus Time

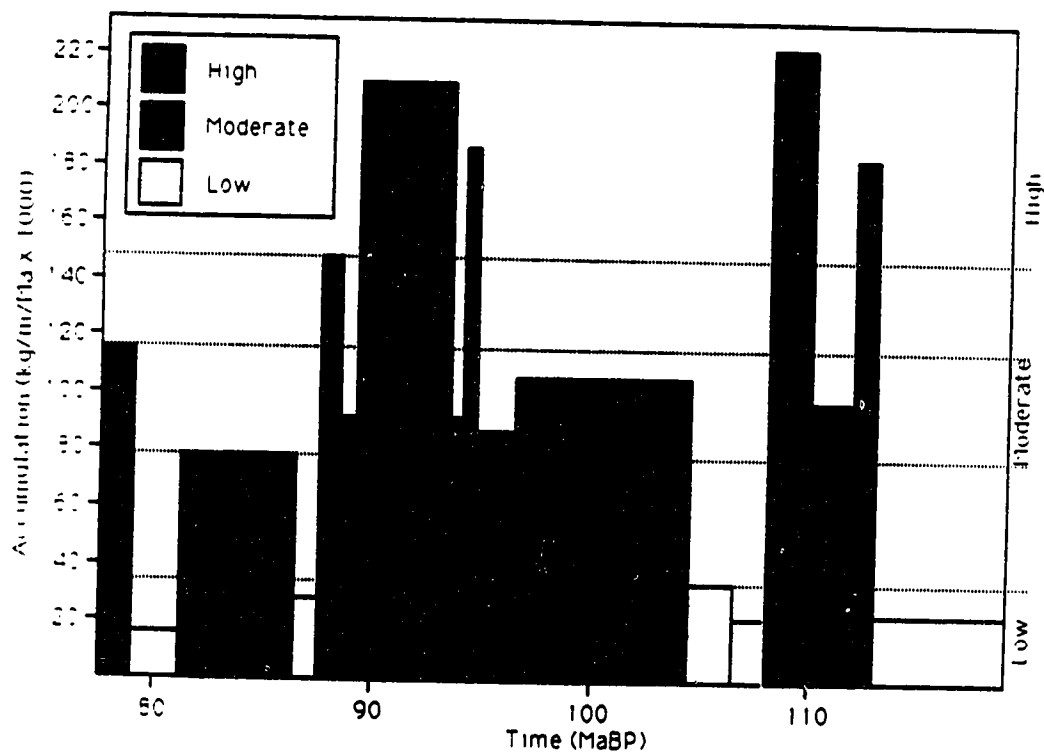


Figure 16. Plot of accumulation rate versus time.



induced rapid sedimentation (Bluesky Formation and Upper Spirit River Group). The rapid deformation was interrupted by a short period of relative quiescence (Lower Spirit River Group). The first cycle terminated in the lower Albian with a return to quiescence in the Cordillera, and the deposition of the Peace River Group. The Shaftesbury and Dunvegan Formations were deposited during the moderate deformation of the second cycle. Then, a series of three pulses of rapid deformation corresponding to the Lower Kaskapau, Upper Kaskapau, and Muskiki Formations occurred. The pulses were separated by short intervals of relative quiescence (Doe Creek and Cardium Formations). The second cycle lasted until the end of the Coniacian, when the Cordillera returned to a period of quiescence.

Each cycle consists of a period of low to moderate deformation followed by rapid deformation. In each cycle the rapid deformation episode has a duration approximately half of that of the preceding phase of low to moderate deformation. The first cycle has a rapid deformation episode representing 3.1 Ma and is preceded by 6.0 Ma of relative quiescence. The second cycle has a rapid deformation episode lasting 6.1 Ma and is preceded by quiescence lasting 13.7 Ma. The third cycle shows only the initial period of quiescence, as most of the strata representing the final episode of rapid deformation were eroded. The magnitude of this erosion has been estimated to be on the order of 2 km (Magara 1978) which suggests that the Paskapoo Formation represents the rapid deposition associated with the culmination of deformation during the third cycle.

Each episode of rapid deformation is interrupted by short intervals of quiescence, shorter than the bounding periods of active

deformation. The two major episodes of deformation, on a finer scale, consist of a series of pulses ranging from 0.5 to 4.4 Ma. This range is similar to that of two pulses of deformation (1.0 and 0.5 Ma duration) observed in the Potwar region of the Himalayas (Johnson *et al.* 1986). This suggests, both in the Canadian Cordillera and the Himalaya, that intense deformation can only be sustained for short periods of time.

Individual pulses within a deformation episode start in localized areas and expand to encompass large areas of the Cordillera. The final pulses of deformation may return to more localized source regions before giving way to relative quiescence. This pattern is the result of tectonism being initiated locally, building to a culmination involving a large area with severe deformation, and waning to less intense deformation in localized areas. For example, the Lower Kaskapau Formation represents the first pulse of deformation in the second episode, and the source area is restricted to a narrow zone between 55° and 56°N (Figure 11b). The second pulse in this episode is represented by the Upper Kaskapau Formation which shows a continuous source region along its western margin (Figure 12b). The accumulation rate for the Upper Kaskapau Formation ( $210 \times 10^3 \text{ kg/m}^2/\text{Ma}$ ) is greater than that for the Lower Kaskapau Formation ( $186 \times 10^3 \text{ kg/m}^2/\text{Ma}$ ). The final pulse in the second episode is represented by the Muskiki Formation which has only a localized source region in the south, and an accumulation rate of  $149 \times 10^3 \text{ kg/m}^2/\text{Ma}$ , as deformation wanes.

Johnson *et al.* (1986) have dated two deformation intervals in the Potwar region of the Himalayas to last from 4.5 to 3.5 MaBP and 2.1 to 1.6 MaBP respectively. The second deformation interval has a duration

of 0.5 Ma and is preceded by 1.4 Ma of relative quiescence. This closely follows the 2:1 ratio of quiescence to deformation formulated from the Canadian Cordillera, on a smaller scale. The deformation intervals of Johnson *et al.* (1986) resemble pulses of deformation within a single deformation episode, as seen in the Canadian Cordillera. If this interpretation is valid, a 4 to 6 Ma period of relative quiescence should be present prior to the rapid deformation. Further investigations are required in order to confirm the existence of the preceding period of low to moderate deformation.

In the Peace River Arch area, the period of quiescence prior to the first deformation cycle is somewhat longer than expected, due to the establishment of a convergent tectonic regime. The Fernie Group represents the extended period of low to moderate sedimentation during which deformation takes place on attenuated continental crust and is accommodated mostly below sea level (Stockmal and Beaumont, 1987). The cyclic nature of Cordilleran deformation and the quantification of active and passive phases can be used to interpolate deformation for time periods where data is missing.

#### B. PREDICTIONS ARISING FROM THE OBSERVED CYCLES

The foreland basin began during the early to mid-Jurassic as the result of deformation along the newly-formed convergent plate boundary. The Jurassic portion of the sedimentary record may contain extensive unconformities, which would result in lower-than-expected calculated mass accumulation rates. In order to attain accumulation rates in the order of  $200 \times 10^3 \text{ Kg/m}^2/\text{Ma}$  (expected for rapid deformation) the Jurassic

isopach would have to be two orders of magnitude thicker than observed (200 m). An isopach of 20 km is unlikely when compared to maximum burial depths indicating only 2 km of erosion since maximum burial (Magara, 1978). The Jurassic is therefore characterized by at most moderate, and more likely low, sediment accumulation. This supports Stockmal and Beaumont's (1987) suggestion that initial deformation adjacent to a foreland basin is accommodated mostly below sea level.

Similarly, erosion has removed much of the sedimentary record since the late Campanian. The moderate deformation calculated up to the Upper Puskwaskau time is assumed to have prevailed until approximately 70 MaBP, when the Pacific Plate changed direction (Kononov, 1984) and the western margin of North America was placed in a transpressive tectonic regime (Monger, 1984). The period from the start of Badheart time to 70 MaBP is approximately 20 Ma, of both moderate deformation and relative quiescence. Based on the observed 2:1 ratio of duration for quiescence versus rapid deformation, the following 10 - 12 Ma represented the final major period of deformation (Laramide Orogeny). This deformation resulted in the rapid deposition of the thick Paleocene Paskapoo Formation. The estimate of 70 to 58 MaBP for rapid deformation from this study is in good agreement with Monger's (1984) estimate for the timing of the Laramide Orogeny and the development of the thrust-fold belt (late-Cretaceous to early Tertiary).

### C. DEFORMATION AND LITHOLOGY

Porter *et al.* (1981) inferred that coarse-grained sediment such

as sand and gravel within the foreland basin can normally be associated with periods of deformation in the adjacent Cordillera, while fine grained mud and silt are associated with periods of quiescence. Graham *et al.* (1986) observed that the lithology of foreland basin sediment in southwestern Montana is controlled by source rock lithology rather than the intensity of deformation in the adjacent thrust-fold belt. The mass accumulation rates calculated in the Peace River Arch area support this assumption. The first episode of rapid accumulation is marked by the deposition of the Bluesky and Upper Spirit River sands. However, the second episode of rapid accumulation coincides with the deposition of the Lower Kaskapau, Upper Kaskapau, and Muskiki shale units, for which the volume of sediment and the time span of each unit necessitates rapid deposition.

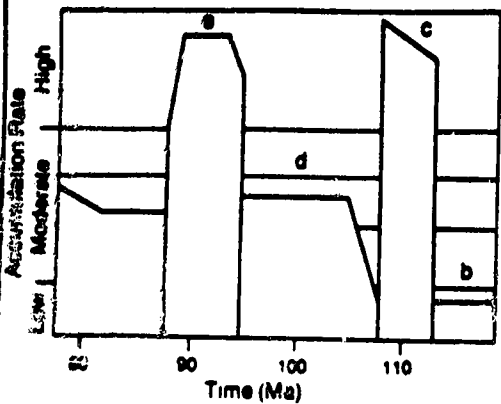
Middle to late Cordilleran deformation involves the uplift of basinal sediment. If a mudstone or shale unit is uplifted and exposed to erosion, the resulting clastic sediment will be a shale. In addition, as mudstone and shale are less resistant, they are more susceptible to rapid erosion: it is reasonable to expect that material eroded rapidly from the deformed belt will accumulate rapidly in the adjacent basin. Therefore, shale units can represent intervals of rapid accumulation throughout the rock record, and may be associated with periods of deformation in an adjacent orogen. Shale deposition associated with deformation suggests that other paleoenvironmental interpretations based strictly on rock type need to be reexamined.

#### D. MODEL OF TECTONIC DEVELOPMENT

A model of tectonic development can be formulated from the mass accumulation rate patterns and magnitudes.

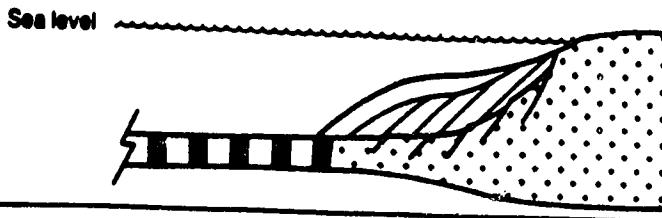
From Cambrian to middle Jurassic, the western North American craton was a passive margin dominated by carbonate deposition (Figure 17a). From middle Jurassic to early Albian, foreign terranes, including the composite Intermontane Superterrane (Monger, 1984), began to accrete loosely along the western margin of the Canadian craton (Figure 17b). This resulted in moderate to low topographic relief, and the shedding of Fernie and Bullhead Group sediment eastward along the entire length of the study area. Within the study area, the initial stage of deformation represented by the Fernie Group was not associated with moderate to high accumulation rates, as most of the deformation was accommodated below sea level on the outboard edge of the continental lithosphere (Stockmal and Beaumont, 1987). From early to mid-Albian, an outboard shift in the subduction zone (Figure 17c) gave rise to an initial pulse of deformation along the length of the study area, followed by a short period of quiescence, and a second pulse of rapid deformation in the southwest part of the study area. The first pulse of deformation resulted in the deposition of the Bluesky Formation. The period of quiescence is indicated by the lower accumulation rate of the Lower Spirit River Group. The second pulse of deformation renewed rapid sediment accumulation with the Upper Spirit River Group. For the next 4.5 Ma deformation all but ceased, leaving minor sedimentation mostly from easterly sources. The accumulation rate patterns for the Lower and Upper Peace River Groups show probable

Generalized Accumulation Rate versus Time

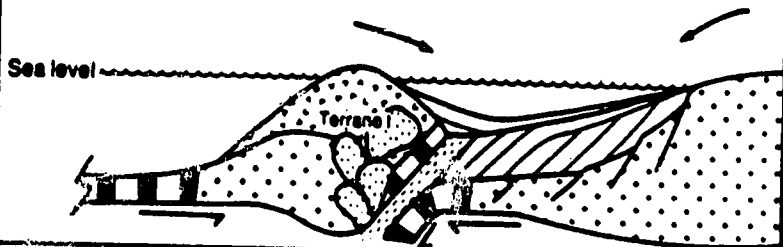


Low Moderate High

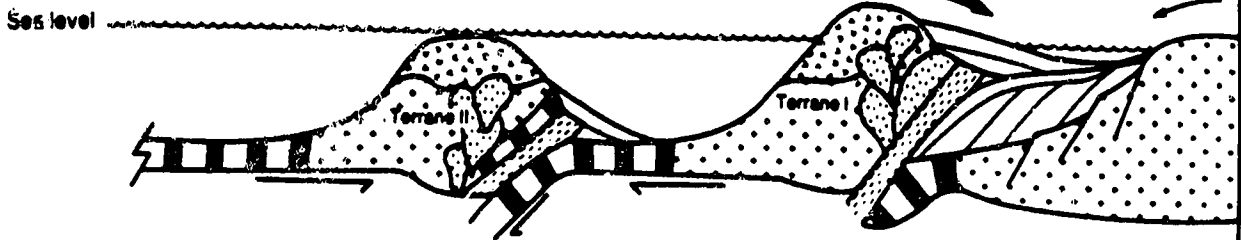
a) 206 Ma



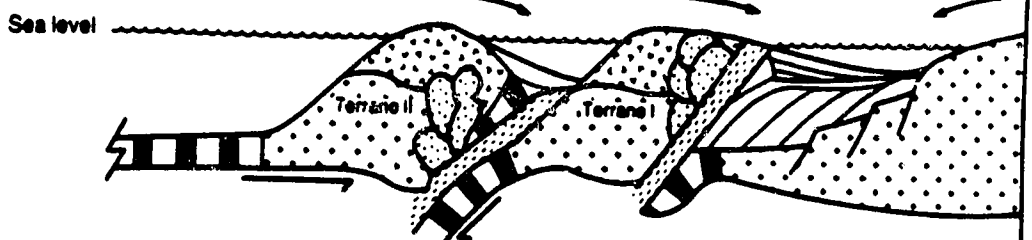
b) 187 Ma



c) 112 Ma



d) 100 Ma



e) 90 Ma



f) 60 Ma

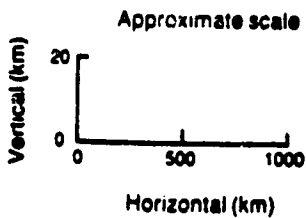
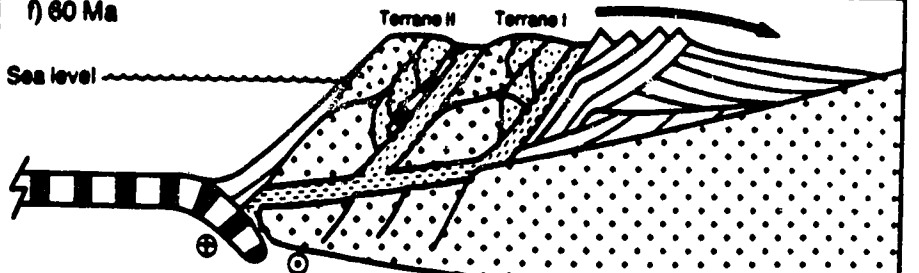


Figure 17. Schematic diagram indicating the six main phases of deformation undergone by the northern Canadian Cordillera.

easterly source regions dominating (Figure 9b and 10a). Until mid-Cenomanian, only moderate deformation occurred as more foreign terranes, including the composite Insular Superterrane (Monger 1984), docked at the western continental margin (Figure 17d). During this period, initial topographic relief in the north gave rise to moderate accumulation (Shaftesbury Formation, Figure 8b); deformation then migrated to a west-central position as indicated by the accumulation pattern of the Dunvegan Formation (Figure 11a). From mid-Cenomanian to late Coniacian, an outboard shift of the subduction zone, resulted in rapid deformation (Figure 17e). Deformation occurred in three pulses separated by short periods of quiescence. The first pulse was located in the west-central part of the study area (Lower Kaskapau Formation, Figure 11b). The second pulse was both more intense and more widespread (Upper Kaskapau Formation, Figure 12b). The third pulse was less intense and more localized, confined to the southwest part of the study area (Muskiki Formation, Figure 13b). Low to moderate deformation continued in localized areas of the Cordillera until late Maastrichtian. At 70 MaBP, the Pacific Plate changed to a northerly direction of movement (Kononov, 1984). The new transpressive regime in the Cordillera shuffled the newly accreted terranes northward, along and further onto the edge of the continental margin (Monger, 1984). The transpression and impingement of terranes lead to the development of the thrust-fold belt (Figure 17f). The final period of rapid deformation (Laramide Orogeny), which lasted throughout the Paleocene, resulted in deposition of the Paskapoo Formation.

Cant and Stockmal (1989) have linked six discrete clastic wedges in the Alberta Foreland Basin to the accretion of two large composite



terrane and four smaller discrete terranes in the Cordillera. Their interpretation is qualitative in the sense that the sedimentary response to deformation is not quantified, and only the geometry and lithology of each clastic wedge is considered in conjunction with estimates for the timing of terrane accretion. The accumulation rate maps developed here complement the results of Cant and Stockmal. Following the accretion of the Intermontane Superterrane during the mid-Jurassic, Cant and Stockmal (1989) inferred the Bridge River terrane docked between Aptian and mid Albian, and the Cascadia terrane during the Cenomanian. Cant and Stockmal (1989) proposed that the accretion of the Insular Superterrane took place during the mid-Campanian, followed by the Pacific Rim-Chugach terrane. The accumulation rate patterns suggest that even though the Intermontane Superterrane docked initially in the Jurassic, a significant sedimentary response in the foreland basin within the study area was not seen until late Albian; this could coincide with Cant and Stockmal's (1989) interpretation of the accretion of the Bridge River terrane, which provides the mechanism of outboard shifting of the subduction zone resulting in rapid deformation as described in this thesis. The accumulation rates indicate that major deformation resulting from the accretion of the Insular Superterrane occurred during the Turonian, somewhat earlier than proposed by Cant and Stockmal (1989). Monger *et al.* (1982) support a mid-Cretaceous accretion time based on geological evidence within the Cordillera.

## 9. CONCLUSIONS

Foreland basin deposits in the Peace River Arch area can be classified into three groups based on the magnitude of their rate of mass accumulation. The first have magnitudes greater than  $148 \times 10^3 \text{ kg/m}^2/\text{Ma}$ , the second have magnitudes between  $73 \times 10^3$  and  $115 \times 10^3 \text{ kg/m}^2/\text{Ma}$ , and the third have magnitudes less than  $35 \times 10^3 \text{ kg/m}^2/\text{Ma}$ . When the mass accumulation rates are arranged on an absolute time scale, a cyclic pattern of deformation can be observed. A single cycle lasts on the order of 25 Ma, and consists of a period of quiescence, a period of moderate deformation, and a period of rapid deformation. The period of rapid deformation is approximately half the duration of the preceding periods of quiescence and moderate deformation combined. The rapid deformation occurs as a series of pulses ranging from 0.5 to 4.4 Ma in duration, which are separated by typically shorter periods of quiescence.

Two complete cycles of deformation and part of a third are preserved for the Cordillera of northern Alberta and adjacent British Columbia. The first cycle begins in the Aptian with the deposition of the Bullhead Group. Rapid deformation results in the deposition of the Bluesky Formation and Upper Spirit River Group. Lower and Upper Peace River Group sedimentation is dominated by easterly source regions during quiescence at the beginning of the second deformation cycle. The second cycle shows moderate deformation until mid-Cenomanian, when rapid deformation ended the cycle with the deposition of the Lower Kaskapau, Upper Kaskapau and Muskiki Formations.

During an episode of rapid deformation, pulses of rapid

deformation tend to initiate locally and expand in both area and intensity to involve larger portions of the deformed belt. Finally, deformation wanes to localized areas, before giving way to a period of quiescence. The Lower Kaskapau, Upper Kaskapau, and Muskiki units collectively show the building and waning trends during a rapid deformation period.

The Fernie Group represents a period of low sediment accumulation rate ( $<35 \times 10^3$  kg/m<sup>2</sup>/Ma) even though it marks the start of Cordilleran deformation. This confirms the observation of Stockmal and Beaumont (1987) that initial stages of deformation result in only low rates of sedimentation because most of the deformation is accommodated below sea level on attenuated continental lithosphere.

During the first deformation cycle, the culmination of deformation led to the rapid deposition of the Bluesky and Upper Spirit River sand dominated units. However, rapid deformation in the deformed belt was not always associated with the deposition of a sand unit. The second cycle shows rapid deformation which resulted in the accumulation of the Lower Kaskapau, Upper Kaskapau, and Muskiki shale-dominated units. The source rock controls the lithology of sedimentation in the adjacent basin. The assumption that sand units are deposited during periods of deformation and shale units are deposited during periods of quiescence is thus invalid in the Peace River Arch study area. Graham *et al.* (1986) observed source rock control on sediment lithology in southwestern Montana, which is in agreement with the relationships between deformation and sedimentation described in this study.

The cyclic nature of continental scale convergent tectonism and the relationship between periods of low to moderate deformation and

rapid deformation in the northern Canadian Cordillera can be compared to the Himalayas. Johnson *et al.* (1986) described periods of low deformation followed by major deformation in the Potwar region. The major deformation periods, of 1.0 and 0.5 Ma durations separated by 1.4 Ma of relative quiescence, are analogous to pulses of deformation within a single deformation episode described for the northern Canadian Cordillera.

## 10. REFERENCES

- Bachu, S., C.M. Sauveplane, A.T. Lytviak, and B. Hitchon, 1987. Analysis of Fluid and Heat Regimes in Sedimentary Basins: Techniques for Use with Large Data Bases. the Am. Ass. Petrol. Geol. Bull., v. 71, No. 7, pp. 822-843.
- Beaumont, C., 1981. Foreland Basins. Geophysical Journal of the Royal Astronomical Society, v. 65, pp. 291-329.
- Bird, P., 1978. Finite Element Modeling of Lithosphere Deformation: The Zagros Collision Orogeny. Tectonophysics, v. 50, pp. 307-336.
- Cant, D.J., and G.S. Stockmal, 1989. The Alberta Foreland Basin: Relationship Between Stratigraphy and Cordilleran Terrane-Accretion Events. Canadian Journal of Earth Science, v. 26, pp. 1964-1975.
- Davies, G.R., 1986. Table of Formations of Alberta. Energy Resources Conservation Board of Alberta.
- Eisbacher, G.H., M.A. Carrigy, and R.B. Campbell, 1974. Paleodrainage patterns and late-orogenic basins of the Canadian Cordillera, in Dickinson, W.R., ed., Tectonics and Sedimentation. Society of Economic Paleontologists and Mineralogists special publication 22, pp. 143-166.
- England, P., 1982. Some Numerical Investigations of Large Scale Continental Deformation, in Hsu, ed., Mountain Building Processes. Acadian Press, pp. 129-139.
- Guidish, T.M., I. Lerche, C.G.St.C. Kendall, and J.J. O'Brien, 1984. Relationship between Eustatic Sea Level Changes and Basement Subsidence. Bull. Am. Ass. Petrol. Geol., v. 68, pp. 326-337.
- Hall, R.L., 1984. Lithostratigraphy and Biostratigraphy of the Fernie Formation (Jurassic) in the southern Canadian Rocky Mountains, in Stott, D.F., and D.J. Glass, eds., The Mesozoic of Middle North America. Can. Soc. of Petrol. Geol. Memoir 9, pp. 233-247.
- Harland, W.B., A. Cox, P.G. Llewellyn, C.A.G. Pickton, A.G. Smith, R. Walters, and K.E. Fancett, 1982. Geologic Time Scale. Cambridge University Press, Cambridge.
- Johnson, G.D., R.G.H. Reynolds, and D.W. Burbank, 1986. Late Cenozoic tectonics and sedimentation in the north-western Himalayan foredeep: I. Thrust ramping and associated deformation in the Potwar region, in Allen, P.A., and P. Homewood, eds., Foreland Basins. International Association of Sedimentologists, special publication 8, pp. 273-291.
- Jordan, T.E., 1981. Thrust Loads and Foreland Basin Evolution, Cretaceous, Western United States. The American Association of Petroleum Geologists Bulletin, v. 65, No. 12, pp. 2506-2520.

- Kauffman, E.G., 1977. Geological and Biological Overview: Western Interior Cretaceous Basin. *The Mountain Geologist*, v. 14, pp. 75-99.
- Kent, D.V., and F.M. Gradstein, 1985. A Cretaceous and Jurassic Geochronology, *Geol. [BSoc. of Amer. Bull.]*, v. 96, pp. 1419-1427.
- Kononov, M.V., 1984. The absolute movement of the Pacific Plate During the last 129 million years. *Oceanology*, 24, 3, p. 368-375.
- Magara, K., 1978. *Compaction and Fluid Migration: Practical Petroleum Geology*. Elsevier, New York, 319 p.
- Monger, J.W.H., 1984. Cordilleran Tectonics: a Canadian Perspective. *Bull. Soc. Geol. France*, (7) XXVI, No. 2, pp. 255-278.
- Monger, J.W.H., R.A. Price, and D.J. Tempelman-Kluit, 1982. Tectonic accretion and the origin of the two major metamorphic and plutonic belts in the Canadian Cordillera. *Geology*, v. 10, pp. 70-75.
- Palmer, A.R., 1983. The Decade of North American Geology 1983 Geologic Time Scale. *Geology*, v. 11, p. 503-504.
- Pate, C.R., 1986. Cretaceous Compaction and Tectonic Subsidence of the Alberta Basin. MSc. Thesis, University of Alberta.
- Porter, J.W., R.A. Price, and R.G. McCrossan, 1982. The Western Canada Sedimentary Basin. *Phil. Trans. R. Soc. Lond. A*, v. 305, pp. 169-192.
- Puigdefabregas, C., J.A. Munoz, and M. Marzo, 1986. Thrust belt development in the eastern Pyrenees and related depositional sequences in the southern foreland basin, in Allen, P.A., and P. Homewood, eds., *Foreland Basins*. International Association of Sedimentologists, special publication 8, pp. 229-246.
- Sampson, R.J., 1978. Surface II Graphics System. No 1, Series on Spatial Analysis, Computer services section, Kansas Geological Survey, Lawrence, Kansas.
- Stockmal, G.S., 1984. Modeling of Large-Scale Accretionary Wedge and Thin-Skinned Thrust-and-Fold Belt Mechanics. Phd. Thesis, Brown University.
- Stockmal, G.S., and C. Beaumont, 1987. Geodynamic Models of Convergent Margin Tectonics: The Southern Canadian Cordillera and the Swiss Alps, in Beaumont, C., and A.J. Tankard, eds., *Sedimentary Basins and Basin Forming Mechanisms*. Can. Soc. of Petrol. Geol. Memoir 12, pp. 393-411.
- Tankard, A.J., 1986. On the depositional response to thrusting and lithospheric flexure: examples from the Appalachian and Rocky Mountain Basins, in Allen, P.A., and P. Homewood, eds., *Foreland*

Basins. International Association of Sedimentologists, special publication 8, pp. 369-392.

Turcotte, D.L., 1980. Models for the Evolution of Sedimentary Basins, in Bally, A.W., P.L. Bender, T.R. McGetchin, and R.I. Walcott, eds., Dynamics of Plate Interiors. Geodynamics Series, v. 1, A.G.U., Washington, pp. 83-97.

Watts, A.B., G.D. Karner, and M.S. Steckler, 1982. Lithospheric Flexure and the Evolution of Sedimentary Basins. Phil. Trans. R. Soc. Lond. A, v. 305, pp. 249-281.

## 11. APPENDIX A

This appendix contains an example of the stratigraphic picks data derived from geophysical logs for the Upper Puskwaskau Formation. Regional geologic data are to be published in an Alberta Research Council open file report (1990).

The land location is organized as:

Township	three spaces
Meridian	one space
Range	two spaces
Section	two spaces
Legal sub division	two spaces,

for the Dominion Land Survey System in Alberta.

The land location is organized as:

Grid Area	one space
Block	three spaces
Unit	one space
Primary quadrant	three spaces
Secondary quadrant	one space
Tertiary quadrant	two spaces,

for the National Topographic System in British Columbia.



## Stratigraphic Picks for the Upper Puskwaskau Formation

Land Location	KB	Elevation
0585011607000	703.8	298.8
0585022206000	665.4	231.4
0585031814000	659.1	214.1
0585042507000	670.2	207.2
0585051606000	669.9	164.9
0585061711000	666.6	124.1
0585072710000	677.6	89.3
0585081802000	738.8	78.8
0585092006000	731.8	32.3
0585101811000	845.5	-23.2
0585113211000	833.9	-28.4
0585131416000	781.2	-113.8
0585142611000	946.1	-154.5
0585151606000	1006.6	-196.4
0585161706000	1039.7	-246.6
0585172506000	1159.5	-245.6
0585181011000	1122.3	-338.3
0585192606000	1090.7	-374.3
0585203311000	977.8	-409.0
0585212206000	988.2	-461.7
0585222711000	998.5	-509.3
0585231510000	1019.0	-586.0
0585241011000	1074.1	-651.1
0585251313000	1047.6	-653.2
0586013408000	1273.0	-749.0
0586042011000	1479.1	-774.9
0586051115000	1592.3	-810.7
0595010506000	721.2	295.7
0595052311000	663.4	190.7
0595061909000	682.2	157.2
0595072305000	700.3	130.3
0595082906000	820.5	102.7
0595113210000	690.1	21.1
0595121811000	715.1	-59.1
0595133610000	780.0	-39.6
0595141806000	974.3	-136.7
0595151511000	988.2	-139.6
0595163104000	975.4	-164.6
0595173407000	937.1	-212.9
0595180906000	1074.7	-273.1
0595192906000	991.2	-337.1
0595212016000	1076.9	-419.1
0595220613000	1182.8	-495.2
0595241907000	1189.9	-581.6
0595252010000	1078.7	-794.3
0595272306000	1196.1	-658.9
0596012906000	1277.0	-699.0
0596052206000	1436.2	-800.8
0596063412000	1368.2	-721.8
0605013310000	623.2	373.2
0605022307000	641.9	332.8
0605040606000	668.4	223.4

0605093005000	748.6	88.7
0605100310000	667.0	71.0
0605112811000	818.4	40.2
0605122106000	792.8	-41.7
0605133310000	878.7	-38.7
0605143507000	787.0	-42.1
0605160511000	905.9	-151.8
0605173604000	840.0	-136.0
0605182006000	927.5	-223.5
0605202511000	922.9	-297.2
0605211110000	995.8	-356.0
0605220706000	1107.0	-409.4
0605233306000	1072.3	-407.5
0605241106000	1046.3	-479.7
0605250412000	1144.7	-593.3
0605270313000	1272.7	-934.3
0606010311000	1301.7	-634.3
0606021111000	1308.4	-657.6
0606052212000	1282.3	-693.7
0615012111000	637.0	384.0
0615051210000	685.2	266.2
0615062411000	659.3	232.3
0615072906000	726.6	202.3
0615081008000	703.2	165.2
0615092906000	766.9	138.7
0615100111000	758.5	116.5
0615113611000	840.6	105.6
0615125010000	844.9	46.3
0615131115000	770.7	7.7
0615143007000	877.6	-17.4
0615152310000	880.6	-64.3
0615160707000	869.9	-70.4
0615172310000	945.5	-109.1
0615183607000	880.6	-111.4
0615192212000	920.2	-209.1
0615203210000	860.6	-244.3
0615210916000	963.7	-258.3
0615222807000	930.2	-314.8
0615231411000	1063.4	-338.4
0615251607000	1140.9	-450.2
0615262806000	1157.6	-405.4
0615272211000	1200.0	-461.0
0616011103000	1243.4	-581.6
0616022813000	1144.6	-543.4
0616030306000	1193.6	-631.4
0616043307000	1102.5	-593.7
0616051306000	1041.4	-639.6
0616062706000	1092.8	-617.2
0616093608000	1177.7	-533.3
0625022807000	643.6	372.6
0625042607000	692.8	345.9
0625051711000	651.2	252.2
0625061604000	644.3	246.3
0625072202000	716.9	243.9
0625082906000	791.6	212.5
0625091411000	797.7	169.2
0625101806000	907.7	126.2
0625122808000	953.7	93.6

0625163006000	973.4	-22.6
0625172610000	932.4	-64.3
0625182110000	876.9	-124.4
0625191812000	895.5	-152.7
0625203204000	822.1	-167.9
0625211011000	843.1	-229.8
0625220710000	890.9	-243.0
0625231107000	1005.2	-287.2
0625242011000	1009.2	-295.8
0625252110000	894.0	-328.2
0625263115000	941.7	-362.3
0625272507000	1054.6	-365.8
0626013411000	1058.7	-391.3
0626023214000	1052.2	-453.8
0626032902000	952.0	-479.0
0626042211000	1071.5	-542.5
0626052406000	929.0	-526.0
0626062307000	1101.9	-522.1
0626071807000	1270.7	-556.6
0626072507000	1183.9	-494.1
0626080907000	1379.2	-456.8
0626092806000	1448.4	-419.6
0635021816000	650.7	415.7
0635041610000	646.4	358.4
0635081512000	833.4	239.4
0635092716000	894.6	232.6
0635112616000	1044.5	176.5
0635120402000	1029.0	111.6
0635133006000	1033.5	107.5
0635143506000	1026.6	107.6
0635151309000	922.8	-7.2
0635160313000	1022.9	-33.1
0635173110000	812.6	-30.2
0635180115000	892.1	-53.9
0635191014000	797.3	-110.7
0635200813000	796.4	-148.5
0635210111000	842.7	-167.3
0635223203000	827.4	-164.6
0635232906000	877.4	-217.6
0635242207000	858.6	-230.1
0635253408000	924.2	-228.9
0635260114000	878.1	-325.9
0635271202000	1003.6	-348.4
0635271407000	940.8	-328.2
0636012013000	970.7	-345.3
0636021312000	990.6	-379.2
0636032009000	968.3	-421.7
0636053006000	1039.9	-424.1
0636060403000	1132.5	-482.5
0636072510000	1031.7	-428.3
0636080207000	1072.4	-453.6
0636091807000	1460.0	-401.0
0636101906000	1278.7	-406.3
0645021310000	624.8	421.8
0645032505000	581.5	396.5
0645041006000	643.8	358.8
0645061211000	770.6	306.7
0645072611000	826.0	318.0

0645111912000	1039.7	187.8
0645123104000	1070.5	117.1
0645133614000	1092.5	142.5
0645141109000	1102.2	52.2
0645152306000	1021.9	41.9
0645160410000	921.4	37.5
0645182802000	768.7	12.8
0645192207000	746.5	-70.4
0645202006000	823.0	-28.9
0645213611000	772.1	-31.9
0645220807000	823.2	-132.8
0645231610000	806.8	-127.1
0645241710000	881.8	-166.7
0646012210000	915.3	-250.0
0646022406000	857.9	-276.2
0646033510000	860.1	-288.9
0646041506000	887.3	-353.2
0646050810000	985.3	-370.7
0646061010000	960.2	-414.8
0646082506000	1046.3	-350.7
0646102908000	1403.1	-229.9
0646111609000	1499.9	-222.1
0655042706000	667.5	406.0
0655053306000	737.3	369.7
0655063311000	785.8	358.5
0655072914000	861.4	332.9
0655093603000	1005.8	314.8
0655103504000	1047.3	206.1
0655112803000	1089.8	230.8
0655132910000	1070.3	190.3
0655141404000	1215.8	143.8
0655152909000	946.7	129.7
0655161113000	1049.2	135.2
0655173610000	800.2	72.2
0655182911000	858.8	53.8
0655192106000	790.2	40.2
0655203310000	741.8	36.8
0655211406000	780.3	-326.7
0655220107000	786.1	-54.2
0655232010000	787.0	-82.5
0655242113000	885.0	-42.0
0655252704000	837.6	-101.2
0655272510000	927.9	-155.1
0656010611000	823.4	-183.6
0656033407000	779.1	-236.2
0656041603000	867.1	-247.9
0656050406000	831.1	-313.9
0656063410000	908.0	-250.0
0656073206000	1029.0	-248.0
0656082910000	1099.0	-268.0
0656102710000	957.7	-179.5
0665060406000	783.6	183.1
0665070106000	788.6	353.6
0665111408000	1116.4	281.4
0665130413000	1164.5	219.5
0665141112000	1163.7	160.9
0665150616000	919.6	133.2
0665163304000	852.5	186.5

0665201815000	706.0	48.0
0665213508000	756.4	79.4
0665222004000	760.0	36.0
0665233207000	769.3	37.3
0665241110000	905.3	-15.2
0665252910000	707.1	-14.1
0665261801000	800.6	-89.4
0666011014000	863.4	-121.6
0666020709000	785.2	-151.8
0666032203000	785.0	-148.0
0666042807000	763.5	-152.5
0666050906000	922.9	-222.1
0666052910000	826.9	-172.8
0666073011000	833.3	-169.5
0666083007000	893.5	-150.5
0666091910000	972.7	-169.3
0666101811000	884.5	-174.5
0666112610000	833.8	-156.2
0675082910000	1006.4	420.3
0675093410000	981.5	402.4
0675111910000	1239.0	332.2
0675151712000	993.4	213.0
0675161712000	951.6	214.0
0675173507000	1006.1	238.0
0675192414000	767.5	173.1
0675200604000	766.1	89.1
0675213516000	705.2	148.2
0675220816000	717.0	92.0
0675232706000	736.3	136.3
0675243116000	755.3	77.3
0675261116000	765.4	18.6
0675273606000	806.5	78.0
0676031814000	809.2	-76.8
0676043108000	580.9	-30.1
0676052010000	713.8	-78.7
0676063211000	760.0	-78.0
0676073310000	757.3	-84.7
0676080706000	868.1	-87.9
0676091410000	851.8	-87.2
0676112510000	841.7	-87.3
0676121407000	842.1	-49.9
0685061307000	805.0	463.6
0685111710000	1230.5	354.9
0685120802000	1236.6	339.0
0685122907000	1054.0	359.1
0685161310000	961.3	220.6
0685180907000	811.4	206.4
0685192811000	795.5	222.5
0685203605000	754.7	222.7
0685213606000	707.9	208.9
0685223207000	700.7	190.5
0685232511000	725.4	158.5
0685240903000	756.1	121.1
0685252014000	686.4	187.4
0685262901000	670.9	142.9
0686011712000	733.0	59.1
0686022606000	674.8	59.1
0686030706000	718.0	2.0

0686072408000	708.9	-23.1
0686090110000	833.0	-37.0
0686102206000	737.4	32.4
0686111606000	766.2	7.2
0686120711000	858.0	27.0
0686131615000	924.9	92.9
0695051207000	782.4	532.5
0695073007000	1078.1	505.7
0695131711000	831.5	390.8
0695143010000	801.6	382.8
0695153010000	841.6	363.1
0695160610000	851.3	293.5
0695182901000	939.1	274.6
0695191509000	784.9	269.9
0695211409000	708.4	252.7
0695222607000	649.8	256.0
0695232709000	740.7	234.7
0695242807000	746.5	204.6
0695251907000	772.1	195.1
0696042510000	544.1	115.1
0696053506000	657.2	132.2
0696061614000	661.5	63.5
0696072806000	683.6	92.6
0696080311000	735.3	31.3
0696093111000	645.3	135.3
0696101010000	723.0	59.0
0696113007000	753.8	103.8
0696123207000	771.5	191.5
0696132307000	834.4	164.4
0705051311000	783.0	558.0
0705090206000	788.4	493.4
0705100602000	880.9	437.7
0705112312000	894.0	438.0
0705122304000	802.8	467.5
0705132604000	763.9	467.9
0705182210000	807.4	361.2
0705193104000	767.2	346.6
0705202116000	687.5	331.5
0705220811000	718.4	277.4
0705230815000	715.7	257.7
0705240710000	751.6	240.1
0705261801000	654.1	250.2
0706011411000	553.8	241.1
0706020904000	640.7	184.7
0706033409000	631.3	193.3
0706051306000	639.0	175.0
0706061006000	673.1	135.1
0706072304000	662.5	154.5
0706081106000	683.4	139.4
0706092206000	709.0	174.0
0706100106000	697.0	142.0
0706111511000	717.5	190.8
0706123311000	768.7	255.7
0706133410000	860.4	304.4
0706141207000	876.3	333.8
0715103111000	794.0	570.3
0715133004000	844.3	494.4
0715141411000	738.2	419.2

0715250906000	701.8	295.8
0716012508000	632.0	312.0
0716032906000	636.4	264.5
0716043114000	679.9	299.9
0716051706000	653.0	242.0
0716060302000	664.7	192.7
0716072808000	750.0	282.0
0716082506000	729.7	293.7
0716092806000	756.9	285.9
0716110311000	728.1	240.1
0716123606000	824.6	347.6
0716133510000	828.5	392.5
0725143607000	732.7	574.2
0725171811000	716.3	463.3
0725182306000	715.4	410.6
0725252011000	813.6	408.6
0726010607000	633.4	339.4
0726032704000	668.2	362.2
0726051708000	683.3	331.3
0726061016000	681.4	316.4
0726073106000	680.8	450.8
0726083406000	705.1	410.1
0726090214000	933.6	332.6
0726100710000	748.2	366.2
0726113006000	743.3	418.3
0726123606000	760.0	446.0
0726130807000	861.9	436.9
0735260719000	728.2	417.3
0736011007000	678.6	412.6
0736040604000	703.8	392.9
0736050110000	685.7	394.7
0736061103000	715.8	410.8
0736070311000	680.4	443.4
0736081811000	740.1	467.1
0736100414000	788.5	442.5
0745012910000	699.2	562.0
0746061306000	778.2	474.6
0755042810000	947.0	671.2
0755050713000	877.1	664.1
0756050408000	861.4	545.4
0756130505000	819.2	714.2
0765022510000	805.9	614.5
0765043010000	778.5	626.1
0785161001000	673.5	545.5
A003B093P0104498	-1000.0	-1639.0
A010A093P1003231	-1000.0	-2021.1
A023I093P0105425	-1000.0	-1477.0
A043B093P0805315	-1000.0	-1355.0
B002H093P0106361	-1000.0	-1540.0
B046H093P0805330	-1000.0	-1235.0
B066L093P0106600	-1000.0	-1357.0
B071J093P0806170	-1000.0	-1052.0
C012A093P0805388	-1000.0	-1378.0
D015D093P0806394	-1000.0	-1319.0
D015H093P0705494	-1000.0	-1241.0
D035E093P0805307	-1000.0	-1205.0
D051J093P0103698	-1000.0	-1477.0
D053G093P0805534	-1000.0	-1210.0

0068K093P0105408

-1000.0 -1387.0

76



## 12. APPENDIX B

This appendix contains an example of core analysis data. The data are arranged per formation and have been vertically averaged. The data includes an arithmetic average and a weighted arithmetic average for both porosity and density. The entire data set is available through the Alberta Geological Survey, a department of the Alberta Research Council, PO Box 8330, Postal Station F, Edmonton Alberta Canada, T6H 5X2.

The land location is organized as:	Township	three spaces
	Meridian	one space
	Range	two spaces
	Section	two spaces
	Legal sub division	two spaces.

for the Dominion Land Survey System in Alberta.

The column headings are as follows:

Por. Ave.	Vertically averaged porosity.
Por. Wgt. Ave.	Vertically averaged weighted porosity.
Den. Ave.	Vertically averaged grain density.
Den. Wgt. Ave.	Vertically averaged weighted grain density.

## Upper Puskwaskau Formation

Land Location	X	Y	Fm #	Unit #	Por Ave	Por Wgt Ave	Den Ave	Den Wgt Ave
0585142906	54.3730	4.6918	4500	93	0.105	0.107	2571.5	2668.1
0586021610	40.0942	4.0317	4500	93	0.050	0.052	2831.1	2842.9
0595012106	67.1055	6.2132	4500	93	0.171	0.170	2718.4	2714.0
0595013511	67.4057	6.5989	4500	93	0.155	0.155	1651.9	2622.0
0605011110	67.4230	6.9246	4500	93	0.215	0.223	2640.6	2639.4
0615020407	66.0697	7.6024	4500	93	0.125	0.125	2540.0	2652.0
0616072810	35.1701	7.2402	4500	93	0.078	0.084	2704.1	2733.1
0625032600	65.2729	9.1705	4500	93	0.158	0.158	2668.7	2670.0
0625041206	64.4950	8.6322	4500	93	0.162	0.162	2693.6	2700.0
0625042506	64.4637	9.1175	4500	93	0.130	0.141	2652.8	2661.0
0625043606	64.4534	9.2780	4500	93	0.163	0.168	2292.5	2734.5
0626073205	34.9277	8.3315	4500	93	0.122	0.139	2732.0	2739.5
0635010410	66.9009	9.6462	4500	93	0.134	0.228	1067.6	2601.7
0635041007	64.1208	9.5811	4500	93	0.107	0.108	2630.4	2628.3
0635041610	63.9448	9.7733	4500	93	0.145	0.129	2670.2	2673.3
0645120612	57.6355	10.0645	4500	93	0.196	0.201	2608.0	2789.6
0645121110	57.5531	10.0604	4500	93	0.173	0.179	2336.7	2765.5
0645121412	56.9839	10.0327	4500	93	0.127	0.126	2437.7	2660.0
06451211102	57.3862	10.1327	4500	93	0.173	0.190	2213.4	2746.7
0645121408	56.4396	10.2904	4500	93	0.099	0.104	2649.5	2653.1
0645121411	56.3573	10.3268	4500	93	0.170	0.170	2398.0	2666.7
0645122210	56.2272	10.4817	4500	93	0.170	0.181	1736.9	2715.7
0645122310	56.3900	10.4893	4500	93	0.149	0.166	2454.6	2699.5
0645122908	55.9363	10.5909	4500	93	0.130	0.135	2720.8	2731.5
0645132310	55.4134	10.4445	4500	93	0.119	0.123	2653.0	2657.2
0645133407	55.2381	10.7203	4500	93	0.146	0.144	2680.8	2682.1
0645133414	55.1944	10.7988	4500	93	0.123	0.124	2657.8	2660.0
0645133510	55.3989	10.7677	4500	93	0.115	0.114	2674.9	2678.7
0645133608	55.6036	10.7367	4500	93	0.076	0.030	2634.4	2640.3
0645133610	55.5616	10.7750	4500	93	0.099	0.099	2641.1	2641.7
0746121814	29.7707	19.6076	4500	93	0.132	0.132	2680.0	2680.0